

GAN YEN SHING

B. Sc. (Hons.) Chemistry

2011

**SYNTHESIS AND CHARACTERISATION OF SMECTIC AND
NEMATIC PHASES IN 4-(DIMETHYLAMINO)BENZYLIDENE-4'-
ALKANOYLOXYANILINES**

GAN YEN SHING

BACHELOR OF SCIENCE (HONS.) CHEMISTRY

FACULTY OF SCIENCE

UNIVERSITI TUNKU ABDUL RAHMAN

APRIL 2011

**SYNTHESIS AND CHARACTERISATION OF SMECTIC AND
NEMATIC PHASES IN 4-(DIMETHYLAMINO)BENZYLIDENE-4'-
ALKANOYLOXYANILINES**

By

GAN YEN SHING

A project report submitted to the Department of Chemical Science,

Faculty of Science,

Universiti Tunku Abdul Rahman,

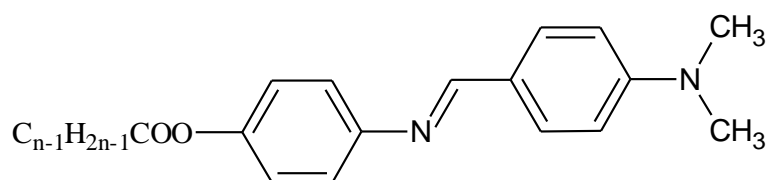
in partial fulfillment of the requirements for the degree of

Bachelor of Science (Hons) Chemistry

May 2011

ABSTRACT

A series of Schiff base esters, 4-(dimethylamino)benzylidene-4'-alkanoyloxylanilines (**nDMABAA**) containing different length of alkanoyloxy chain ($C_{n-1}H_{2n-1}COO-$, $n = 6, 8, 10, 12, 14, 16, 18$) at end of the molecules have been successfully synthesized.



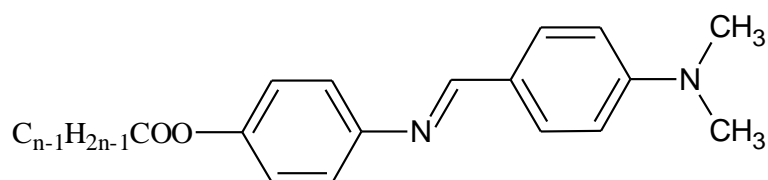
nDMABAA

where $n = 6, 8, 10, 12, 14, 16, 18$

The structure of the compounds were elucidated by using Fourier transform infrared (FTIR) spectroscopy, nuclear magnetic resonance (1H and ^{13}C NMR) spectroscopy and electron-ionisation mass spectrometry (EI-MS). The mesomorphic properties of these compounds were studied by using polarising optical microscope (POM) attached to a Linkam hostage and differential scanning calorimeter (DSC). All the compounds exhibited monotropic properties whereby the liquid crystal phases were only observed during cooling cycle. Lower derivatives ($n = 6, 8$ and 10) exhibited only nematic phase, medium derivative ($n = 12$) exhibited co-existence of both nematic and smectic A phases and higher derivatives ($n = 14, 16$ and 18) only exhibited smectic A phase. The structure-mesomorphic relationship within the series and structurally related series reported in the literature were also discussed.

ABSTRAK

Satu siri sebatian hablur cecair, 4-(dimetilamino)benzalidena-4'-alkanoiloksi-anilina (**nDMABAA**) yang mempunyai rantai alkaniloksi dengan kepanjangan yang berbeza ($C_{n-1}H_{2n-1}COO-$, $n = 6, 8, 10, 12, 14, 16, 18$) di salah satu hujung molekul telah berjaya disintesiskan.



nDMABAA

di mana $n = 6, 8, 10, 12, 14, 16, 18$

Semua struktur sebatian ini telah dikenalpastikan dengan menggunakan kaedah spektroskopi inframerah (IR), spektroskopi resonans magnetik nucleus (1H and ^{13}C NMR) dan elektron-pengionan spektrometrik jisim (EI-MS). Ciri-ciri hablur cecair telah dikaji dengan menggunakan mikroskop optical berkutub (POM) yang beroperasi bersama pentas pemanasan Linkam dan kalorimeter pengimbasan perbezaan (DSC). Semua sebatian memaparkan sifat monotropik di mana fasa hablur cecair hanya wujud semasa proses penyejukan. Sebatian ($n = 6, 8$ dan 10) menunjukkan hanya fasa nematik, sebatian ($n = 12$) menunjukkan fasa nematik dan smektik A dan sebatian ($n = 14, 16, 18$) menunjukkan hanya fasa smektik A. Hubungan antara struktur molekul dan ciri-ciri hablur cecair dalam siri ini serta struktur berkaitan yang dilaporkan dalam literatur juga telah dibincangkan.

ACKNOWLEDGEMENTS

This final year project would not have been possible without the support of many people. First of all, I owe my deepest gratitude to my project supervisor, Assistant Professor Dr. Ha Sie Tiong who was abundantly helpful and offered me invaluable support and guidance throughout the duration of this project.

I am grateful to Professor Dr. Yeap Guan Yeow of Universiti Sains Malaysia (USM) and his postgraduate students for their collaboration in carrying out the POM analysis on some of my compounds. I also want to share my appreciation to National University of Singapore (NUS) for providing me the technical support in analyzing the compounds.

Next, I would like to express my appreciation to Faculty of Science of Universiti Tunku Abdul Rahman for providing all the supports to complete this project. High appreciation goes to all laboratory officers for their assistance. I also want to give my thankfulness to my seniors, Mr. Foo Kok Leei and Mr. Lee Teck Leong for their guidance. Their enthusiasm and perpetual energy in research had motivated me in working hard to complete the project.

Last but not least, I would like to thank my teammates and others post graduate students who are sharing the same laboratory with me. This is such a great and memorable experience to work together with them.

APPROVAL SHEET

I certify that, this project report entitled **“SYNTHESIS AND CHARACTERISATION OF SMECTIC AND NEMATIC PHASES IN 4-(DIMETHYLAMINO)BENZYLIDENE-4’-ALKANOYLOXYANILINES”** was prepared by **GAN YEN SHING** and submitted in partial fulfillment of the requirements for the degree of Bachelor of Science (Hons.) in Chemistry at Universiti Tunku Abdul Rahman.

Approved by

Supervisor

(Dr. Ha Sie Tiong)

Date:

FACULTY OF ENGINEERING AND SCIENCE
UNIVERSITI TUNKU ABDUL RAHMAN

Date: _____

PERMISSION SHEET

It is hereby certified that **GAN YEN SHING** (ID. No: **08ANB05471**) has completed this report entitled “**SYNTHESIS AND CHARACTERISATION OF SMECTIC AND NEMATIC PHASES IN 4-(DIMETHYLAMINO)-BENZYLIDENE-4’-ALKANOYLOXYANILINES**” under supervision of **Dr. Ha Sie Tiong** from Department of Chemical Science, Faculty of Science.

I hereby give permission to my supervisors to write and prepare manuscript of these research findings for publishing in any form, if I did not prepare it within six (6) months time from this date provided that my name is included as one of the authors for this article. Arrangement of name depends on my supervisors.

DECLARATION

I hereby declare that project report is based on my original work except for quotations and citations which have been duly acknowledged. I also declare that it has not been previously or concurrently submitted for any other degree at UTAR or other institutions.

GAN YEN SHING

Date:

TABLE OF CONTENTS

	Page
ABSTRACT	i
ABSTRAK	ii
ACKNOWLEDGEMENTS	iii
APPROVAL SHEET	iv
PERMISSION SHEET	v
DECLARATION	vi
TABLE OF CONTENTS	vii
LIST OF TABLES	xi
LIST OF FIGURES	xii
LIST OF ABBREVIATIONS	xv
CHAPTER	
1 INTRODUCTION	1
1.1 Definition of Liquid Crystals	1
1.2 History of Liquid Crystals	3
1.3 Types of Liquid Crystals	5
1.3.1 Thermotropic Liquid Crystals	5
1.3.1.1 Calamitic (Rod-Like) Liquid Crystals	6
1.3.1.2 Discotic (Disc-Like) Liquid Crystals	7
1.3.2 Lyotropic Liquid Crystals	7
1.4 Phase Structures and Textures of Achiral Calamitic Liquid Crystals	9
1.4.1 Nematic Phase	9
1.4.2 Smectic Phase	11
1.5 Structure of Calamitic Liquid Crystals	12

1.6	Objectives of Study	14
2	LITERATURE REVIEW	15
2.1	Schiff Base Liquid Crystals	15
2.2	Structure-Mesomorphic Properties Relationship	16
2.2.1	Influence of Terminal Group on Mesomorphic Properties	16
2.2.2	Influence of Alkyl Chain Length on Mesomorphic Properties	19
2.2.3	Influence of Lateral Group on Mesomorphic Properties	23
2.2.4	Influence of linking Group on Mesomorphic Properties	28
3	MATERIALS AND METHODOLOGY	31
3.1	Chemicals	31
3.2	Synthesis	32
3.2.1	Synthesis of 4-{(4-(Dimethylamino)benzylidene)amino} phenol, DMABAP	33
3.2.2	Synthesis of 4-(Dimethylamino)benzylidene-4'-alkanoyloxyanilines, nDMABAA	33
3.2.2.1	Synthesis 4-(Dimethylamino)benzylidene-4'-hexanoyloxyaniline, 6DMABAA	33
3.2.2.2	Synthesis of 4-(Dimethylamino)benzylidene-4'-octanoyloxyaniline, 8DMABAA	34
3.2.2.3	Synthesis of 4-(Dimethylamino)benzylidene-4'-decanoyloxyaniline, 10DMABAA	34
3.2.2.4	Synthesis of 4-(Dimethylamino)benzylidene-4'-dodecanoyloxyaniline, 12DMABAA	34
3.2.2.5	Synthesis of 4-(Dimethylamino)benzylidene-4'-tetradecanoyloxyaniline, 14DMABAA	35
3.2.2.6	Synthesis of 4-(Dimethylamino)benzylidene-4'-hexadecanoyloxyaniline, 16DMABAA	35

3.2.2.7	Synthesis of 4-(Dimethylamino)benzylidene-4'-octadecanoyloxyaniline, 18DMABAA	35
3.3	Characterisation	36
3.3.1	Thin Layer Chromatography (TLC)	36
3.3.3	Infrared Spectroscopy Analysis	36
3.3.4	¹ H and ¹³ C Nuclear Magnetic Resonance Spectroscopy Analysis	37
3.3.5	Mass Spectrometry Analysis	37
3.3.6	Polarising Optical Microscopy (POM) Analysis	38
3.3.7	Differential Scanning Calorimetry (DSC) Analysis	38
4	RESULTS AND DISCUSSION	39
4.1	Synthesis and Characterization of 4-{(4-(Dimethylamino)-benzylidene)amino}phenol, DMABAP	39
4.1.1	Synthesis Route of 4-{(4-(Dimethylamino)-benzylidene)amino}phenol, DMABAP	39
4.1.2	Mechanism of Schiff Base Formation of DMABAP	40
4.1.3	Infrared Spectral Analysis of starting materials and Intermediate compound, DMABAP	43
4.2	Synthesis and Characterization of 4-(Dimethylamino)-benzylidene-4'-alkanoyloxyanilines, nDMABAA	47
4.2.1	Synthesis Route of 4-(Dimethylamino)benzylidene-4'-alkanoyloxyanilines, nDMABAA	47
4.2.2	Mechanism of Steglich Esterification of nDMABAA	48
4.2.3	Infrared Spectral Analysis of nDMABAA	52
4.2.4	Nuclear Magnetic Resonance Analysis	58
4.2.3.1	¹ H NMR Spectral Analysis of nDMABAA	58
4.2.3.2	¹³ C NMR Spectral Analysis of nDMABAA	62
4.2.4	Mass Spectrometry Analysis of nDMABAA	67
4.3	Mesomorphic Behaviour Analysis	72
4.3.1	Polarising Optical Microscopy Analysis of nDMABAA	72

4.3.2	Differential Scanning Calorimetry Analysis of nDMABAA	76
4.3.3	Effect of Alkyl Chain Length on Mesomorphic Properties	79
4.4	Structural Comparison with Compounds Reported in the Literature	82
5	CONCLUSIONS	85
6	REFERENCE	88

LIST OF TABLE

Table		Page
2.1	Transition temperature of IP-On and BIP-On series (Vora <i>et al.</i> , 2001)	18
2.2	Transition temperature of compounds E-3H , E-3OH , E-3F , E-3CH₃ , E-3Cl and E-2Cl (Al-Hamdani <i>et al.</i> , 2010)	27
2.3	Transition temperature and associated enthalpy changes of series A, B and C (Belmar <i>et al.</i> , 1999)	30
3.1	List of chemicals used in this project	31
4.1	IR spectral data of starting materials and intermediate compound, DMABAP	46
4.2	IR spectral data of 4-dimethylaminobenzaldehyde, palmitic acid and 16DMABAA	55
4.3	IR spectral data of nDMABAA where n = 6, 8, 10, 12, 14, 16 and 18	57
4.4	¹ H NMR data and the proposed structure of 14DMABAA	58
4.5	¹³ C NMR data and the proposed structure of 14DMABAA	62
4.6	m/z value and the proposed fragment of 14DMABAA	67
4.7	Transition temperature and associated enthalpy changes upon heating and cooling of nDMABAA	77
4.8	Comparison of mesomorphic properties among structurally related compounds	82

LIST OF FIGURES

Figure		Page
1.1	Schematic arrangement of molecules in various phases	2
1.2	Structure of cholesteryl benzoate (Dierking, 2003)	4
1.3	Structure of N-(4-Methoxybenzylidene)-4-butylaniline (MBBA) (Dierking, 2003)	6
1.4	Structure of benzene-hexa- <i>n</i> -alkanoates (Chandrasekhar <i>et al.</i> , 1977)	7
1.5	Simplified soap molecule (Parbhoo, 2008)	8
1.6	Micelle formation (Parbhoo, 2008)	8
1.7	Molecular arrangement and thread-like texture of nematic liquid crystal (Dierking, 2003)	10
1.8	Molecular arrangement and fan-shaped texture of smectic A liquid crystal (Dierking, 2003)	11
1.9	Molecular arrangement and broken fan-shaped texture of smectic C liquid crystal (Dierking, 2003)	12
1.10	General structure for calamitic liquid crystals	12
2.1	Structure of 4-decyloxybenzylidene-4'-alkyloxyanilines (Godzwon <i>et al.</i> , 2007)	15
2.2	Structure of 4-alkanoyloxybenzylidene-4'-chloroanilines, nCIAB (Ha <i>et al.</i> , 2010)	20
2.3	Plot of transition temperature versus the length of alkanoyloxy chain of nCIAB during heating cycle (Ha <i>et al.</i> , 2010)	21
2.4	Structure of 2-(4'- <i>n</i> -alkoxyphenylazo)-6-nitrobenzothiazoles nAPNB (Prajapati and Bonde, 2009)	22
2.5	Plot of transition temperature versus the length of alkoxy chain of nAPNB during heating cycle (Prajapati and Bonde, 2009)	22

2.6	Structure of 2[(4-n-alkoxy-benzyloxy)phenyl azomethine]-5-methylthiazole (series A) and 2-[(4-n-alkoxy-benzyloxy)-2-hydroxy salicylamine]-5-methyl thiazole (series B) (Thaker <i>et al.</i> , 2007)	24
3.1	Synthetic scheme of 4-(dimethylamino)benzylidene-4'-alkanoyloxyanilines, nDMABAA	32
4.1	Synthesis route of Schiff base formation for DMABAP	39
4.2	Mechanism of Schiff base formation for DMABAP	42
4.3	IR spectra of starting materials and intermediate compound, DMABAP	45
4.4	Synthesis route of Steglich esterification for nDMABAA	47
4.5	Mechanism of Steglich esterification for nDMABAA	49
4.6	1,3-Rearrangement of O-acylisourea to N-acylurea	50
4.7	Reaction route of DMAP	51
4.8	IR spectra of 4-dimethylaminobenzaldehyde, palmitic acid and 16DMABAA	54
4.9	IR spectra of nDMABAA where n = 6, 8, 10, 12, 14, 16 and 18	56
4.10	¹ H NMR spectrum of 14DMABAA	59
4.11	¹³ C NMR spectrum of 14DMABAA	63
4.12	EI-mass spectrum of 14DMABAA	68
4.13	Mechanism of fragmentation for [N(CH ₃) ₂ -C ₆ H ₄ -CH=N-C ₆ H ₄ -OH] ⁺ ion	69
4.14	Mechanism of fragmentation for N(CH ₃) ₂ C ₆ H ₄ -CH=N-C ₆ H ₄ ⁺ ion	70
4.15	Mechanism of fragmentation for CH ₃ (CH ₂) ₁₂ -C ⁺ =O ion	70
4.16	Mechanism of fragmentation for N(CH ₃) ₂ -C ₆ H ₄ ⁺ ion	71
4.17	Mechanism of fragmentation for CH ₃ (CH ₂) ₃ ⁺ and CH ₃ (CH ₂) ₂ ⁺ ion	71

4.18	(a) Optical photomicrograph of 10DMABAA exhibiting nematic phase with marble and homeotropic texture during cooling cycle.	74
	(b) Optical photomicrograph of 10DMABAA exhibiting Brownian flashes during cooling cycle.	
4.19	(a) Optical photomicrograph of 12DMABAA exhibiting nematic phase with schlieren and homeotropic (dark area) textures during cooling cycle.	75
	(b) Optical photomicrograph of 12DMABAA exhibiting smectic A phase with focal-conic fan and homeotropic (dark area) textures during cooling cycle.	
4.20	Optical photomicrograph of 14DMABAA exhibiting smectic A phase with focal-conic fan texture during cooling cycle.	75
4.21	DSC thermogram of 14DMABAA	78
4.22	Plot of transition temperature versus the length of alkanoyloxy chain of nDMABAA series during heating cycle	81

LIST OF ABBREVIATIONS

6DMABAA	4-(Dimethylamino)benzylidene-4'-hexanoyloxyaniline
8DMABAA	4-(Dimethylamino)benzylidene-4'-octanoyloxyaniline
10DMABAA	4-(Dimethylamino)benzylidene-4'-decanoyloxyaniline
12DMABAA	4-(Dimethylamino)benzylidene-4'-dodecanoyloxyaniline
14DMABAA	4-(Dimethylamino)benzylidene-4'-tetradecanoyloxyaniline
16DMABAA	4-(Dimethylamino)benzylidene-4'-hexadecanoyloxyaniline
18DMABAA	4-(Dimethylamino)benzylidene-4'-octadecanoyloxyaniline
DMABAP	4-{(4-(Dimethylamino)benzylidene)amino}phenol
DCC	N, N'-Dicyclohexylcarbodiimide
DCM	Dichloromethane
DMAP	4-Dimethylaminopyridine
DMF	Dimethylformamide
DSC	Differential Scanning Calorimetry
FTIR	Fourier Transform Infrared
N	Nematic
NMR	Nuclear Magnetic Resonance
POM	Polarising Optical Microscope
ppm	Parts per million
SmA	Smectic A
SmC	Smectic C
TMS	Tetramethylsilane

CHAPTER 1

INTRODUCTION

1.1 Definition of Liquid Crystals

Liquid crystal is a phase of matter whose order is intermediate between that of a liquid and that of a crystal. The difference between crystal and liquid, the two most common condensed matter phases, is that the molecules in a crystal are ordered whereas in a liquid they are not. The existing order in a crystal is usually both positional and orientational. Positional order refers to the extent to which molecules or group of molecules, on average, show translational symmetry while orientational order refers to the extent to which the molecules align along a specific direction on a long-range basis (Collings, 2002). The molecules in crystal are constrained both to occupy specific sites in a lattice and to point their molecular axes in specific directions. The molecules in liquid, on the other hand, diffuse randomly throughout the sample container with the molecular axes tumbling wildly. As illustrated in Figure 1.1, when a molecular material composed of anisotropic molecules is heated from the solid phase different possibilities exist at the melting point.

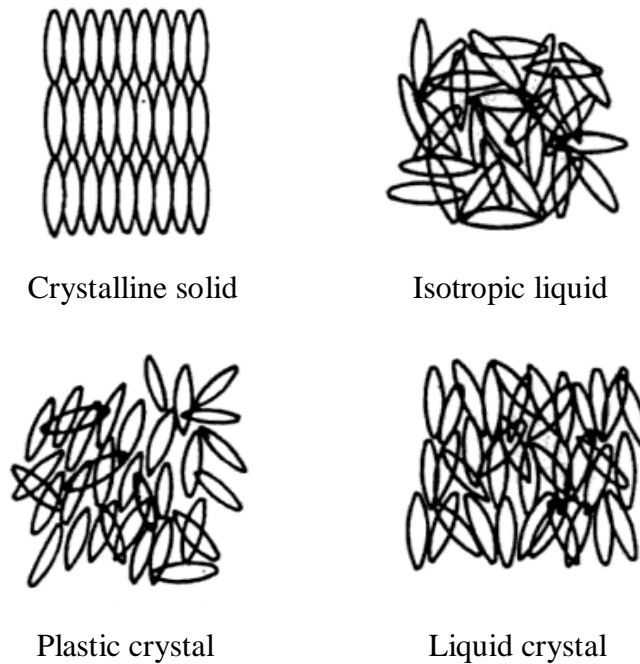


Figure 1.1: Schematic arrangement of molecules in various phases

- i. If both positional and orientational disappear simultaneously, the resulting phase will be an “isotropic liquid”.
- ii. If only orientational order disappears leaving the positional order intact, the resulting phase will be a “plastic crystal”. Materials in this phase exhibit rotator phases; the molecules can rotate along one or more of their molecular axes freely whereas their centers of mass are fixed in a lattice.
- iii. If the positional order either fully or partially disappear while some degree of orientational order is maintained, the resulting phase will be a “liquid crystal” which also called mesophase (intermediate phase) or mesomorphic phase. In this phase, the unique axes of the molecules remain, on average, parallel to each other, leading to a preferred direction in space.

The molecules in all liquid crystal phases diffuse about much like the molecules of a liquid, but as they do so they maintain some degree of orientational order and sometimes some positional order also. The amount of order in a liquid crystal is quite small relative to a crystal. There is only a slight tendency for the molecules to point more in one direction or to spend more time in various positions than others. The fact that most of the order of a crystal is lost when it transforms to liquid crystal is revealed by the value of the latent heat. Values are around 250 J/g, which is very typical of a crystal to liquid transition. When a liquid crystal transforms to a liquid, however, the latent heat is much smaller, typically about 5 J/g. Yet the small amount of order in a liquid crystal reveals itself by mechanical and electromagnetic properties typical of a crystal (Singh and Dunmur, 2002a).

1.2 History of Liquid Crystals

The discovery of liquid crystal dated back to the year of 1888, when an Austrian botanist Friedrich Reinitzer (1858-1927) who is working at the German University of Prague reported on the observation of compound cholesteryl benzoate (Figure 1.2) with two melting points. Solid cholesteryl benzoate melted to form a cloudy liquid at 145.5 °C and turned into a clear, transparent liquid at 178.5 °C (Collings and Hird, 1998a). He also observed some unusual colour behaviour upon cooling; first a pale blue colour appeared as the clear liquid turned cloudy and second a bright blue-violet colour appeared as the clear liquid

crystallised. Reinitzer had discovered and described three important features of cholesteric liquid crystal (the name coined by Georges Friedel in 1922): the existence of two melting points, the reflection of circularly polarised light, and the ability to rotate the polarisation direction of light. He then sent his early work to a German Physicist named Otto Lehmann who was studying the crystallisation properties of various substances (Stegemeyer, 1994a). Lehmann had constructed a polarising microscope with a stage to control the temperature of his samples precisely. This instrument allowed him to observe the crystallisation of his samples under controlled conditions. With this microscope, he examined Reinitzer's samples and noticed its similarity to some of his own samples. He observed that they flow like liquid and exhibit optical properties like of a crystal. The subsequent studies established that these observed intermediate phases represent a new thermodynamic state of matter that are quite distinct from the isotropic liquid. The mechanical and symmetry properties of these phases are intermediate between those of a crystalline solid and an isotropic liquid. Lehmann first called them "flowing crystals" (1889) or "crystalline solids" (1890) and later used the term of "liquid crystals" (1990) (Mohanty, 2003).

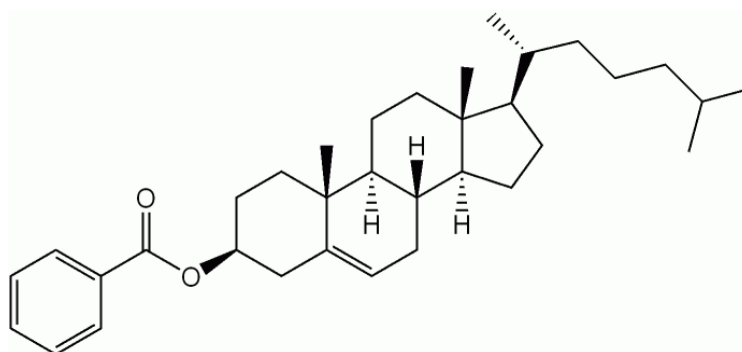


Figure 1.2: Structure of cholesteryl benzoate (Dierking, 2003)

1.3 Types of Liquid Crystals

Liquid crystals are generally divided into two categories: thermotropic liquid crystals and lyotropic liquid crystals. These two types of liquid crystals are distinguished by the mechanisms that drive their self-organization, but they are also similar in many ways.

1.3.1 Thermotropic Liquid Crystals

Thermotropic transitions occur in most liquid crystals, and they are defined by the fact that the transitions to the liquid crystal state are induced thermally. Thermotropic liquid crystals change phase upon heating or cooling. When the mesophase is obtained by heating the crystalline solid as well as by cooling the isotropic liquid, the mesophase is said to be enantiotropic. However, sometime it is only possible to obtain a mesophase by cooling the isotropic liquid, such a mesophase is said to be monotropic. They are only stable in a certain temperature interval. If the temperature is too high, thermal motion will destroy the delicate ordering of the liquid crystal phases, pushing the material into a conventional isotropic liquid phase. However, if the temperature is too low, most liquid crystal materials will form a conventional crystal (Chandrasekhar, 1992).

Thermotropic liquid crystals can be further distinguished with respect to the molecular shape of the constituent molecules, being called calamitic for rod-like and discotic for disk-like molecules.

1.3.1.1 Calamitic (Rod-Like) Liquid Crystals

Calamitic liquid crystals or also known as rod-like liquid crystals are mesogens or mesogenic compounds with elongated shape where one molecular axis is much longer than the other two. A common structural feature of calamitic mesogens is a relatively rigid core, often incorporating phenyl and biphenyl groups, and two flexible terminal groups, often alkyl or alkoxy chains. It is important that the molecule be fairly rigid for a least portion of its length, since it must maintain an elongated shape in order to produce interactions that favour alignment (Collings and Hird, 1998a). Figure 1.3 shows a typical example of calamitic mesogen, N-(4-Methoxybenzylidene)-4-butylaniline (**MBBA**).

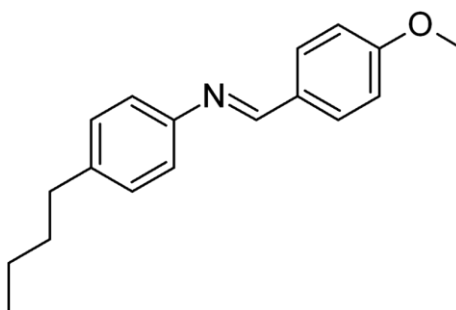


Figure 1.3: Structure of N-(4-Methoxybenzylidene)-4-butylaniline (MBBA) (Kelker and Scheurle, 1969)

1.3.1.2 Discotic (Disc-Like) Liquid Crystals

Discotic liquid crystals or disc-like liquid crystals are mesogens or mesogenic compounds with disc shape where one molecular axis is much shorter than the other two. Rigidity in the central part of the molecules is essential. The core of a typical discotic mesogen is usually based on benzene, triphenylene or truxene, with six or eight side chains, each resembling a typical calamitic mesogen (Collings and Hird, 1998a). Figure 1.4 shows the first discotic liquid crystals, benzene-hexa-*n*-alkanoates reported by Chandrasekhar *et al.* (1977).

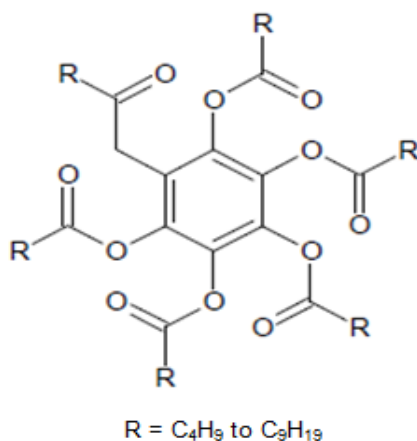


Figure 1.4: Structure of benzene-hexa-*n*-alkanoates (Chandrasekhar *et al.*, 1977)

1.3.2 Lyotropic Liquid Crystals

In contrast to the thermotropic mesophases, lyotropic liquid crystal transitions occur with the influence of solvents in certain concentration ranges, not by a change in temperature. Lyotropic mesophases occur as a result of solvent aggregation of the constituent mesogens into micellar structures. Lyotropic

mesogens are typically amphiphilic, meaning that they are composed of both hydrophilic group at one end and hydrophobic group at the other end. A good example of a lyotropic liquid crystal is soap (Singh and Dunmur, 2002b). As can be seen from Figure 1.5, the soap molecule has a polar “head” group attached to a hydrocarbon “tail” group.

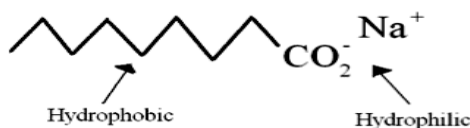


Figure 1.5: Simplified soap molecule (Parbhoo, 2008)

When dissolved in a polar solvent such as water, the hydrophobic “tails” will assemble together as the hydrophilic “heads” extend outward toward the solution to form a micelle structure as shown in Figure 1.6.

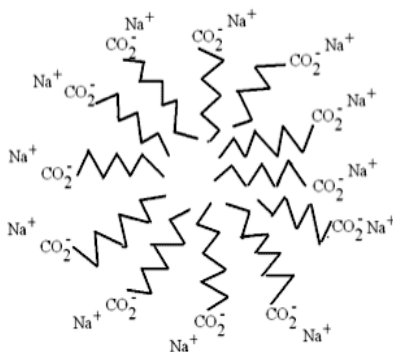


Figure 1.6: Micelle formation (Parbhoo, 2008)

The self-assembled structure depends strongly on the content of water or other solvent molecules. At low amphiphile concentration, the molecules will be dispersed randomly without any ordering. However, as the concentration increases, amphiphilic molecules will spontaneously assemble into micelles and

these micelles will eventually become ordered in the solution as the concentration continues to increase (Fisch, 2006). A typical phase is a hexagonal columnar phase (middle soap phase), where the amphiphiles form long cylinders that arrange themselves into a roughly hexagonal lattice. At some concentrations, the lamellar phase (neat soap phase) forms, where extended sheets of amphiphiles are separated by thin layers of water (Luzzati *et al.*, 1957).

1.4 Phase Structures and Textures of Achiral Calamitic Liquid Crystals

There are many types of liquid crystal phases (mesophases), defined and characterised by many physical parameters such as orientational order (the extent to which the molecules pointing in the same direction) and positional order (the extent to which the molecules are arranged in an ordered lattice), long order (molecules extends to larger dimensions) and short order (molecules are close to each others), and so on. Achiral calamitic mesophases are generally divided into two types: nematic phase and smectic phase.

1.4.1 Nematic Phase

It is the most common liquid crystal phases. The word nematic comes from the Greek word for thread. This term refers to the thread-like defects often observed in micrographs. In this phase, the calamitic molecules have no positional order, but they self-align to have long-range orientational order with their long

axes roughly parallel (Regoa *et al.*, 2010). Thus, the molecules are free to flow and their center of mass positions are randomly distributed as in a liquid, but still point in the same direction referred to the director, n . Most nematics are uniaxial, meaning that they contains one axis that is longer and preferred, with the other two being equivalent. However, some of them are biaxial nematics, meaning that they also orient along a secondary axis besides orienting their long axis (Madsen *et al.*, 2004). Nematics have fluidity similar to that of isotropic liquids but they can be easily aligned by an external magnetic or electric field. Aligned nematics have the optical properties of uniaxial crystals and this makes them extremely useful in liquid crystal displays (Stegemeyer, 1994b). Molecular arrangement and thread-like texture of nematic liquid crystal are shown in Figure 1.7.

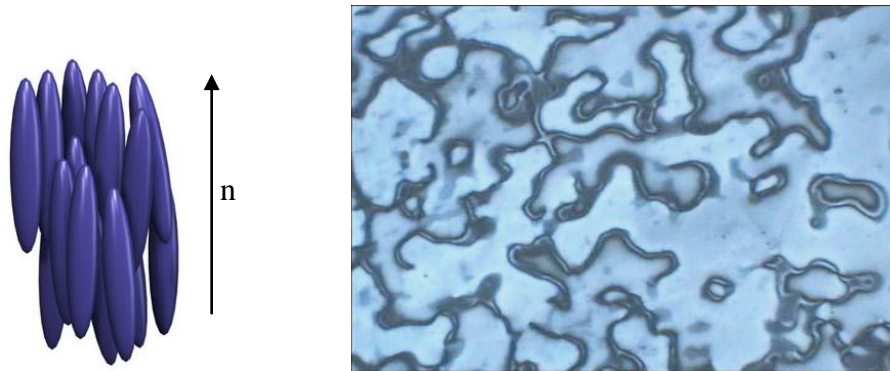


Figure 1.7: Molecular arrangement and thread-like texture of nematic liquid crystal (Dierking, 2003)

1.4.2 Smectic Phase

The word smectic is derived from the Greek word for soap, because at first such liquid crystal phase was observed on ammonium and alkali soaps. Generally, this phase occurs at temperature lower than the nematic, form well-defined layers that can slide over one another like soaps. The smectics are thus positionally ordered along one direction. There are many different smectic phases, all characterised by different types and degrees of positional and orientational order. The most important ones are smectic A and smectic C. In smectic A, the director n is perpendicular to the planes of the layers whereas in smectic C the molecules are tilted with respect to the plane layer (Stegemeyer, 1994a). Molecular arrangement and fan-shaped texture of smectic liquid crystal are shown in Figures 1.8 and 1.9.

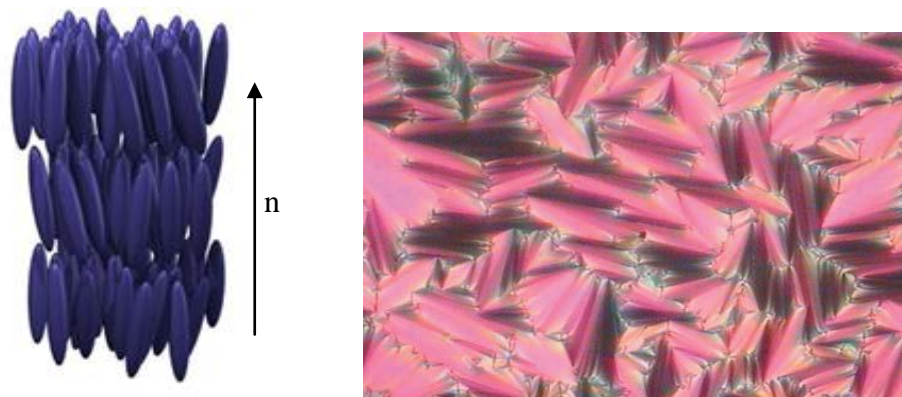


Figure 1.8: Molecular arrangement and fan-shaped texture of smectic A liquid crystal (Dierking, 2003)

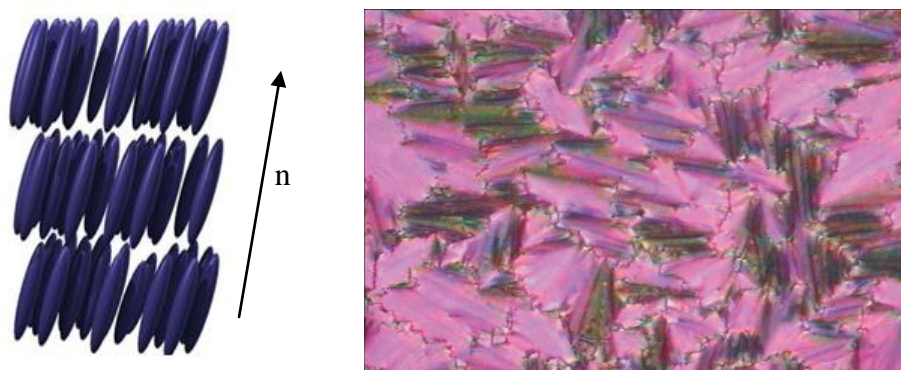


Figure 1.9: Molecular arrangement and broken fan-shaped texture of smectic C liquid crystal (Dierking, 2003)

1.5 Structure of Calamitic Liquid Crystals

Figure 1.10 shows that basic structure of the most commonly occurring liquid crystal molecules.

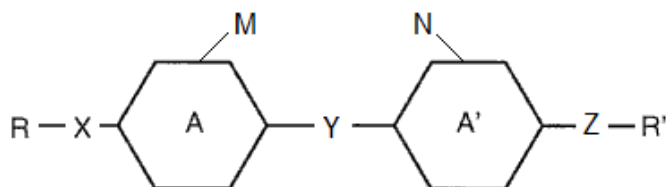


Figure 1.10: General structure for calamitic liquid crystals

A and A' are the core units which are sometimes linked by a linking group Y but more often a direct link is used. Similarly, the terminal chains R and R' can be linked to the core with groups X and Z but usually the terminal chains are directly linked to the core. Lateral substituents M and N are often used to modify the mesophase morphology and the physical properties of liquid crystals to generate enhanced properties for applications. The constituent units within in this general

structure and their combinations determine the type of liquid crystal phase and the physical properties exhibited by a compound (Stegemeyer, 1994a). Certain rigidity is required to provide the anisotropic molecular structure; this core of the structure is usually provided by linearly linked ring systems A and B that are usually aromatic (e.g., 1,4-phenyl, 2,5-pyrimidnyl, 2,6-naphthyl) but can also be alicyclic (e.g., trans-1,4-cyclohexyl). The rings can be directly linked or joined by a linking group Y which maintains the linearity and polarisability anisotropy ($\Delta\alpha$) of the core. Examples of linking group are stilbene ($-\text{CH}=\text{CH}-$), ester ($-\text{CO}_2-$), tolane ($-\text{C}\equiv\text{C}-$), azoxy ($-\text{N}=\text{N}-$), Schiff base ($-\text{CH}=\text{N}-$), acetylene ($-\text{C}\equiv\text{C}-$), and diacetylene ($-\text{C}\equiv\text{C}-\text{C}\equiv\text{C}-$). The names of liquid crystals are often fashioned after the linking group (e.g., Schiff-base liquid crystal). The chemical stability of liquid crystals depends strongly on the central linking group. Schiff base liquid crystals are usually quite unstable while ester, azo, and azoxy compounds are more stable, but also quite susceptible to moisture, temperature change, and ultraviolet radiation. Liquid crystal compounds without a central linking group are normally highly stable (Lam, 2007).

Normally the rigid core alone is not sufficient to generate liquid crystal phases and certain flexibility is required to ensure reasonably low melting point and to stabilize the molecular alignment within the mesophase structure. The flexibility is provided by the terminal substituents R and R' which are usually straight alkyl ($\text{C}_n\text{H}_{2n+1}$) or alkoxy chains ($\text{C}_n\text{H}_{2n+1}\text{O}$); however, one terminal unit is often a small polar substituent (e.g., CN, F, NCS, NO_2). Occasionally, the

terminal chains are branched and the branching unit can be non-polar (e.g., CH₃) or polar (e.g., CN, F, CF₃); this design feature is normally used to introduce chirality into the molecules. Although generally detrimental to the formation of liquid crystal phases, many different types of lateral substituents (e.g., F, Cl, CN, CH₃) are often necessary to tailor their physical properties. The fluoro substituent is the most useful because of its subtle combination of small size and high electronegativity (Collings and Hird, 1998a).

1.6 Objectives of Study

The main objectives of this study are:

1. To synthesize a new series of Schiff base esters 4-(dimethylamino)benzylidene-4'-alkanoyloxyanilines, **nDMABAA**, containing even number of carbons at the end group of the molecules (C_{n-1}H_{2n-1}COO-, n = 6, 8, 10, 12, 14, 16, 18).
2. To elucidate the structure of the title compounds using Fourier transform infrared spectroscopy (FT-IR), nuclear magnetic resonance (NMR) and electron-ionisation mass spectroscopy (EI-MS) techniques.
3. To characterise the liquid crystalline properties of the title compounds using polarising Optical Microscopy (POM) and differential Scanning Calorimetry (DSC) techniques.
4. To study the influence of the alkyl chains, along with their length on the liquid crystalline properties of the title compounds.

CHAPTER 2

LITERATURE REVIEW

2.1 Schiff Base Liquid Crystals

Schiff base or also known as imine (CH=N), a well-known linking group is usually incorporated into the molecular structure to extend the length and polarisability anisotropy of the molecular core to enhance the stability and range of liquid crystal phase (Singh and Dunmur, 2002c). Due to its interesting properties such as rich polymorphism and considerable temperature range of phase transition, extensive studies had been conducted on Schiff bases since the discovery of 4-methoxybenzylidene-4'-butylaniline (**MBBA**) which exhibits a room temperature nematic phase (Kelker and Scheurle, 1969). In addition, Schiff bases with two alkyloxy chains; especially those with long chains are expected to exhibit a rich polymorphism. Godzwon *et al.* (2007) reported a homologous series of 4-decyloxybenzylidene-4'-alkyloxyanilines which exhibit nematic, smectic A, smectic B, smectic C, smectic I and smectic G mesophases.

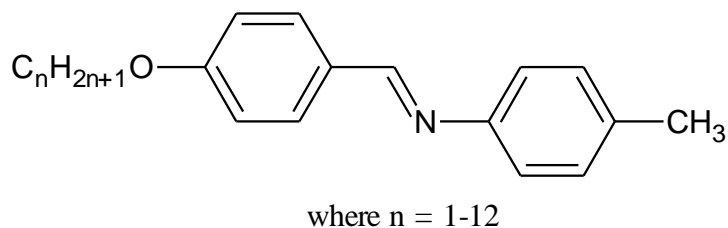


Figure 2.1: Structure of 4-decyloxybenzylidene-4'-alkyloxyanilines (Godzwon *et al.*, 2007)

2.2 Structure-Mesomorphic Properties Relationship

2.2.1 Influence of Terminal Group on Mesomorphic Properties

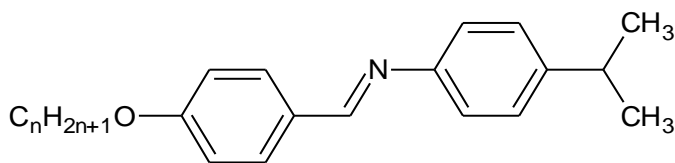
Terminal groups are virtually always employed in liquid crystal systems to adjust mesomorphic properties by creating dipoles along the molecular axis. It has been found that terminally substituted compounds exhibited more stable mesophases as compared to unsubstituted mesogenic compounds (Collings and Hird, 1998b). Generally in a liquid crystalline compound, the terminal groups found such as alkyl and alkoxy chains are unbranched or a compact unit such as CN, NO₂, halogen etc (Galewski and Coles, 1999; Yeap *et al.*, 2006). However a few examples of mesogenic compounds with branched terminal alkyl groups are also known (Vora *et al.*, 2001; Narasimhaswamy and Srinivasan, 2004). Different types of terminal groups tend to have different roles in the generation of liquid crystal phase.

In order to investigate the effect of terminal branching on mesomorphism, Vora *et al.* (2001) have studied the properties of two mesogenic homologous series consisting of an isopropyl terminal group: 4-*n*-alkoxybenzylidene 4'-isopropylanilines, **IP-On** and 4-(4'-*n*-alkoxybenzoyloxy)benzylidene 4''-isopropylanilines, **BIP-On**. The results are shown in Table 2.1. In **IP-On** series, the *n*-octyloxy and *n*-dodecyloxy derivatives exhibit enantiotropic smectic A phase, *n*-decyloxy and *n*-tetradecyloxy derivatives exhibit monotropic smectic A phase whereas rest of the members are non-mesogenic. Lower homologues as

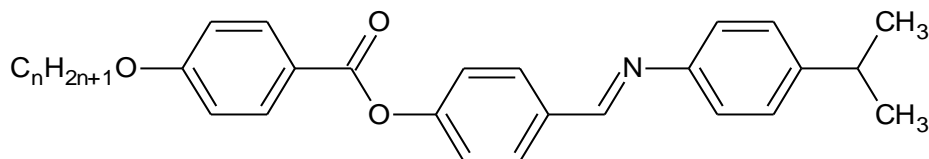
well as higher homologues of this series are non-mesogenic. This indicates that isopropyl terminal group disturbs the molecular order when the molecules do not have sufficient chain length or very long chain length. Yet, the *n*-octyloxy to *n*-tetradecyloxy derivatives are still able to exhibit smectic A phase despite of the presence of isopropyl terminal group.

In **BIP-On** series, enantiotropic nematic phase was observed on all the members while the smectic C phase commenced from the *n*-heptyloxy derivative and was exhibited along with nematic phase until the last *n*-hexadecyloxy derivative studied. It is known that branching in the alkyl chain adjacent to phenyl ring drastically affects the mesomorphic properties of the system. However, if the branching does not have maximum breadth increasing effect, then the deterring effect would be less and in some cases polarisability effect may dominate and thus enhancing the mesomorphic properties. Since this entire series are mesomorphic in nature, this suggests that in this series the branched methyl group does not have maximum breath increasing effect or it finds a pocket in the layer arrangement of smectic phase, whereas its presence on terminus affect the parallel arrangement of molecules which is required to generate nematic phase (Collings and Hird, 1998b).

Table 2.1: Transition temperature of IP-On and BIP-On series
(Vora *et al.*, 2001)



Series IP-On



Series BIP-On

Compound	Transition temperature, °C						
	Cr	→	SmA	→	N	→	I
IP-O1	.	-	-	-	-	71.0	.
IP-O2	.	-	-	-	-	73.0	.
IP-O3	.	-	-	-	-	61.0	.
IP-O4	.	-	-	-	-	66.0	.
IP-O5	.	-	-	-	-	60.0	.
IP-O6	.	-	-	-	-	64.0	.
IP-O7	.	-	-	-	-	58.0	.
IP-O8	.	56.5	.	-	-	59.0	.
IP-O10	.	60.0 ^a	.	-	-	64.0	.
IP-O12	.	54.5	.	-	-	60.0	.
IP-O14	.	64.0 ^a	.	-	-	74.0	.
Compound	Cr	→	SmC	→	N	→	I
BIP-O1	.	-	-	133.0	.	210.0	.
BIP-O2	.	-	-	142.0	.	206.0	.
BIP-O3	.	-	-	154.0	.	200.0	.
BIP-O4	.	-	-	148.0	.	196.0	.
BIP-O5	.	-	-	131.0	.	190.0	.
BIP-O6	.	-	-	124.0	.	186.0	.
BIP-O7	.	108.0	.	118.0	.	182.0	.
BIP-O8	.	114.0	.	126.0	.	176.0	.
BIP-O10	.	110.0	.	137.0	.	168.0	.
BIP-O12	.	110.0	.	145.0	.	162.0	.
BIP-O14	.	85.0	.	149.0	.	157.0	.
BIP-O16	.	82.0	.	145.0	.	153.0	.

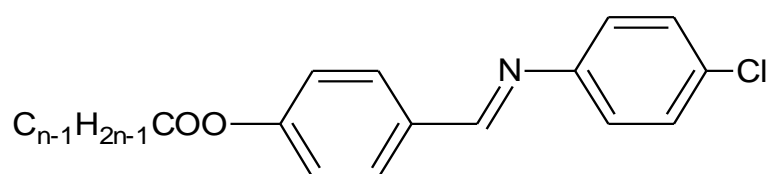
^a indicates monotropic phase

2.2.2 Influence of Alkyl Chain Length on Mesomorphic Properties

In the series of Schiff base esters comprising a polar chloro terminal group, 4-alkanoyloxybenzylidene-4'-chloroanilines, **nCIAB** (Figure 2.2) with different numbers of carbons at the end of the molecules ($C_{n-1}H_{2n-1}COO-$, $n = 2-8$) reported by Ha *et al.* (2010), the first two members (C2 and C3) do not exhibit any mesomorphic properties. The structures of these two molecules with short alkanoyloxy chains are too rigid; therefore have high melting point, thus inhibiting liquid crystal phase formation. As the length of the terminal chain increased, it provides more flexibility to the rigid core structure, hence promoting monotropic SmA and SmB smectic phase in C4 and C6. C5 and C7 members exhibited enantiotropic SmA and SmB phases while C8-C16 members exhibited enantiotropic SmA and monotropic SmB phases. For the highest member of this series, C18 derivative, enantiotropic SmA phase was observed.

The shortest member of this series, C2 derivative possessed the highest melting temperature. The melting temperature decreased as the length of the chain increase to C7 member with exception of C6 member. This happened due to the increase in the flexibility of the molecule induced by the longer alkyl chain. However, from C7 member onwards to C18 member (except C10 member), an increase in the melting temperature was observed due to the increase in the Van der Waals attractive forces between the molecules (Singh and Dunmur, 2002c).

The zig-zag pattern or the odd-even effect was observed in the melting temperatures of the lower members of the homologous series (C4, C5, C6, C7, and C8) as illustrated in Figure 2.3. As the series ascends from the C4 to the C8 member, the Cr-to-SmA/I transition temperatures attenuates consistently. The even members possessed higher clearing temperatures compared to their odd member counterparts. Such trend of the melting temperatures has been observed in various homologous systems of liquid crystals (Demus *et al.*, 1998). While the C4 to C10 members exhibited an increase in their transition temperatures during the SmA-to-I transition, the opposite was observed for the C10 to C18 members. This result revealed that the terminal intermolecular attraction is important in determining the SmA-I transition temperatures. If the attraction becomes weaker, the smectic molecular order will be disrupted, allowing partial interpenetration of the layers to occur more easily as the alkanoyloxy chains length increases, in turn depressing the SmA-to-I transition temperature (Prajapati and Bonde, 2009).



where $n = 2-8, 10, 12, 14, 16$ and 18

Figure 2.2: Structure of 4-alkanoyloxybenzylidene-4'-chloroanilines, nCIAB (Ha *et al.*, 2010)

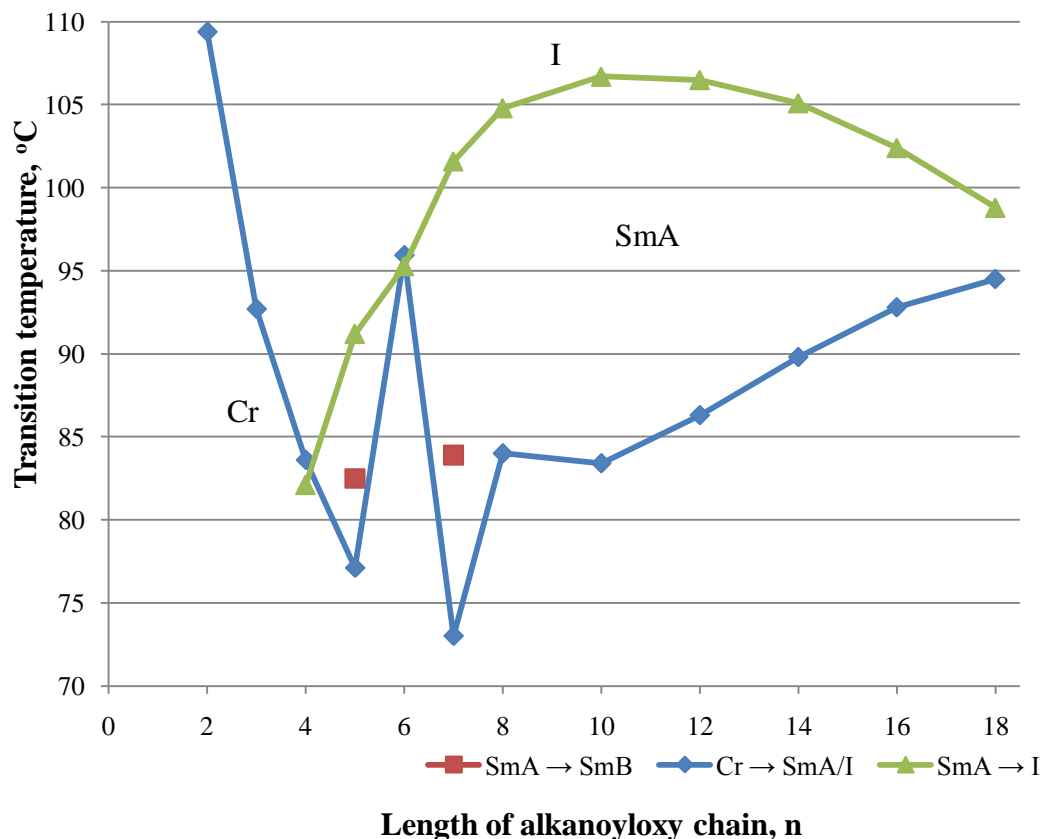
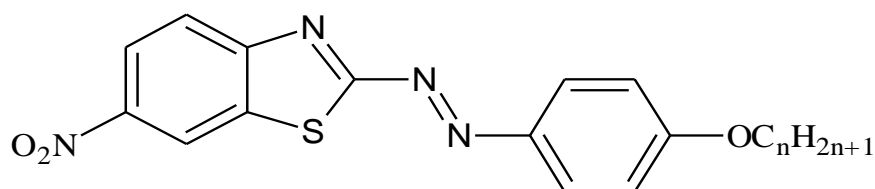


Figure 2.3: Plot of transition temperature versus the length of alkanoyloxy chain of nCIAB during heating cycle (Ha *et al.*, 2010)

Similar mesomorphic properties changes upon the influence of alkyl chains can also be observed in the homologous series containing 6-nitrobenzothiazole moiety at the terminus of the molecule, 2-(4'-n-alkoxy phenylazo)-6-nitrobenzothiazoles, **nAPNB** (Figure 2.4) reported by Prajapati and Bonde (2009). All the nine members in this series are mesogenic and exhibit only the SmA mesophase. The plot of transition temperatures against the number of carbon atom in the alkoxy chain (Figure 2.5) show falling tendency for SmA-I transition and also exhibit usual odd–even effect for lower members, whereas Cr-SmA transition exhibit falling tendency as the series ascended except the ethoxy

derivative. Again, this result revealed that the SmA-I transition temperatures depend greatly on the terminal intermolecular attractions. The depression of SmA-I transition temperatures is due to the partial interpenetration of the layers which happens more easily if the terminal intermolecular attractions become weaker as the alkyl chains become longer.



where $n = 4-8, 10, 12$ and 16

Figure 2.4: Structure of 2-(4'-n-alkoxyphenylazo)-6-nitrobenzothiazoles nAPNB (Prajapati and Bonde, 2009)

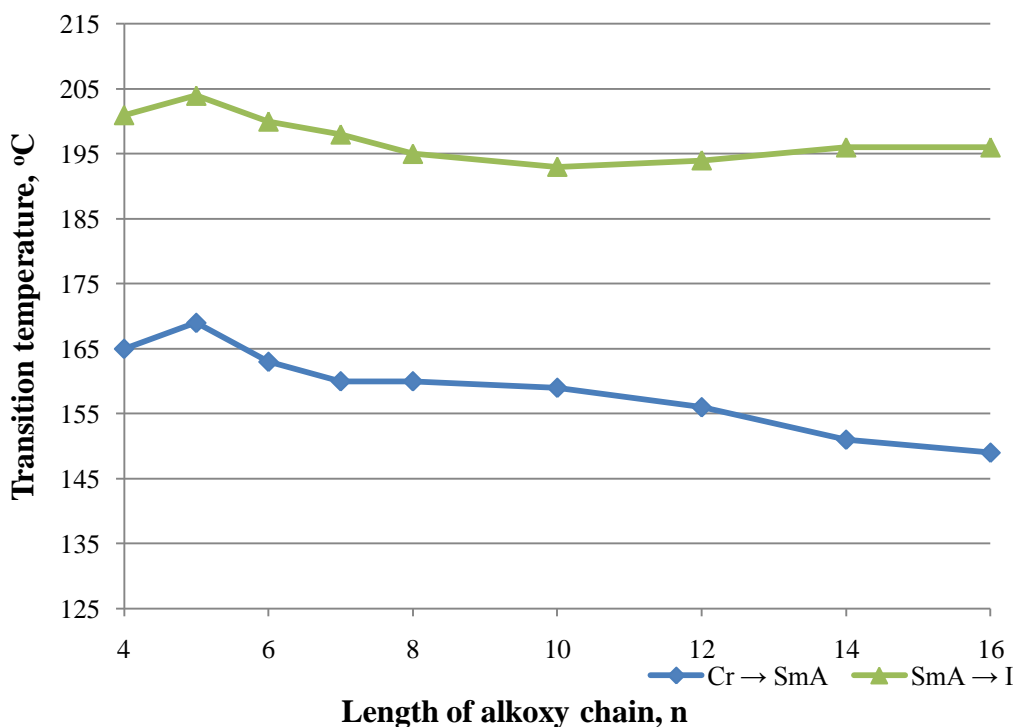


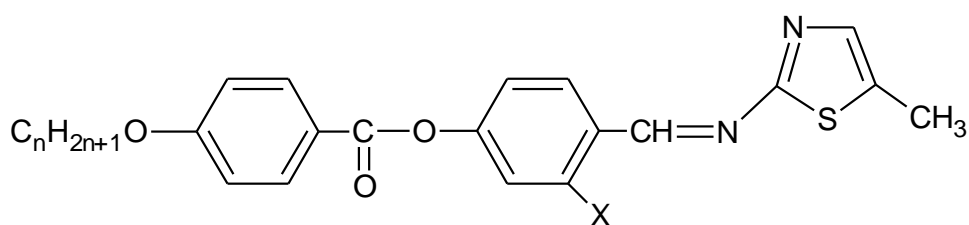
Figure 2.5: Plot of transition temperature versus the length of alkoxy chain of nAPNB during heating cycle (Prajapati and Bonde, 2009)

2.2.3 Influence of Lateral Group on Mesomorphic Properties

Lateral substitution is important in both nematic systems and smectic systems; however, because of the particular disruption to the lamellar packing, lateral substitution to a mesogen always reduces smectic phase stability more than nematic phase stability. It was also generally accepted that the depression of T_{N-I} by a lateral substituent is directly proportional to the size of the substituent irrespective of its polarity. However, the depression of smectic phase stability by a lateral substituent can be partially countered if the lateral substituent is polar; lamellar packing is disrupted by the increased size but enhanced by increased polarity at the same time (Demus *et al.*, 1998).

Such phenomenon can be clearly observed in the study done by Thaker *et al.* (2007) on twelve homologues from each of the two series, 2[(4-n-alkoxybenzyloxy)phenyl azomethine]-5-methylthiazole (series A) and 2-[(4-n-alkoxybenzyloxy)-2-hydroxy salicylamine]-5-methyl thiazole (series B). In this study, series B with a polar hydroxyl group as lateral substitution exhibit the nematic as well as smectic C mesophases, whereas series A with no lateral substitution exhibit only the nematic phase. It is known that compounds with shielded lateral substituents are less effective in molecular broadening. The compounds of series B may give rise to shielding effects owing to the presence of intramolecular hydrogen bonding and hence the polarisability along the long axis of molecules will be larger in such compounds than in the unsubstituted analogue. This results

in higher clearing temperatures than in the corresponding compound in series A without an ortho-hydroxy group. It can therefore be proposed that the introduction of hydroxyl group at the *ortho* position of the aldehyde fragment enhanced the stability of smectic phase, resulting from the increase in Van der Waals forces, which in turn is caused by the increased molecular polarisability anisotropy (Collings and Hird, 1998b).



where X = H in series A, OH in series B

n = 1-8, 10, 12, 14 and 16

Figure 2.6: Structure of 2[(4-n-alkoxy-benzyloxy)phenyl azomethine]-5-methylthiazole (series A) and 2-[(4-n-alkoxy-benzyloxy)-2-hydroxy salicylamine]-5-methyl thiazole (series B) (Thaker *et al.*, 2007)

Such influence of lateral group on mesomorphic properties can also be observed in another study reported by Al-Hamdani *et al.* (2010) on six mesomorphic azo compounds distinguished by the presence of diverse lateral substituents on a central benzene nucleus: compounds **E-3H**, **E-3OH**, **E-3F**, **E-3CH₃**, **E-3Cl** and **E-2Cl** with a general molecular structure as illustrated in Table 2.2. It was found that all the synthesized compounds exhibit enantiotropic. In order to evaluate the effect of the nature and position of the lateral substituents on mesomorphism, the mesomorphic properties of all the substituted compounds were compared with those of the unsubstituted parent compounds.

The probability that a compound exhibit a smectic or nematic mesophase depends on the degree of difference between the terminal and lateral attractions. Smectic phase is most often observed when the lateral to terminal ratio is high while the nematic phase appears when the opposite occurs. Generally, the substitution of the hydrogen at the 2- and 3- positions of azo compounds by Cl, CH₃ and F introduces an additional dipole moment across the long axis of the molecules which enhances the intermolecular lateral attractions and promotes smectic phase for the substituted compounds, but in this case the observed mesophase is nematic. Three possible reasons were suggested for the absence of smectic properties, first: the dipole moment of the substituent is partly cancelled by the dipole of the ester which normally positioned with its C=O group *trans* to the substituted group, second: there is no other dipole acting across the long axis of the molecules. Third: the strength of the intermolecular lateral attractions was reduced as the long narrow molecules were forced further apart due to the increase in molecular breadth (Demus *et al.*, 1998).

For compound **E-2Cl**, the electron withdrawing inductive effect of the chlorine atom is very strong, and is not overwhelmed by the electron releasing resonance effect. Thus, the polar chloro lateral substituent will have a relatively high charge density, identical in sign to that carried by the oxygen atom of the carbonyl moiety of the ester linking group. Repulsion between these two will either cause a reduction in the coplanarity between the carbonyl moiety and the phenyl ring to which it attached, or twist the two phenyl rings out of plane by

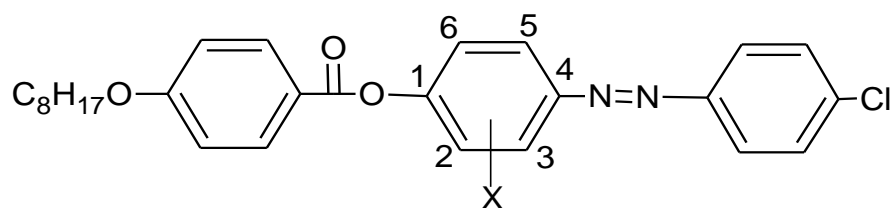
rotation about the phenol ether moiety carbon - oxygen bond. In either event, the nematic thermal stability of the **E-2Cl** molecule will be decreased through the loss of conjugation or thickening of the molecule. For **E-3Cl** molecule, this repulsive situation is alleviated by a 2-chloro substituent lying on the opposite side of the molecule to the carbonyl function, yet the molecular breadth is markedly increased. Again, this will cause a reduction in the N-I transition temperature (Gray *et al.*, 1981).

For compound, **E-3CH₃** the intramolecular hydrogen bonding between the hydroxyl group and the azomethine nitrogen atom gives the molecules a rigid central core in which the aromatic rings adopt an almost coplanar orientation and the polarisability of the molecules is increased, so the effect of the hydroxyl group on the breadth of the molecule is lessened. It can be therefore predicted such structure will prefer nematic phase to a greater degree than the other compounds (Marcos *et al.*, 1983).

In compound **E-3F**, same as the unsubstituted parent compound, smectic and nematic phases were observed at a high temperature range. This similarity indicates that the ratio of lateral to terminal attraction forces of the compound is also as high as other substituted compounds, **E-3CH₃**, **E-3Cl**, **E-2Cl**, despite the influence of the opposite orientation of the dipole moments of the ester and fluoride groups. This is due to the fact that the fluoride atom has a smallest size as compared to other substituents, hence it does not aid in increasing the width of the

molecules. In addition, although C-F bond possessing a high dipole moment that acts through the long axis of the molecule, it cannot be cancelled totally by the dipole moment due to the ester group (Dziaduszek *et al.*, 2009), so the resultant dipole moment along the longitudinal axis of the molecule approaches the resultant dipole moment through the lateral axis of the molecule, causing the terminal attractive forces to be almost the same as the lateral attraction forces and this makes the two phases appear at low temperatures.

Table 2.2: Transition temperature of compounds E-3H, E-3OH, E-3F, E-3CH₃, E-3Cl and E-2Cl (Al-Hamdani *et al.*, 2010)



where 3X = H, OH, Cl, CH₃
2X = Cl

Compound	Transition temperature, °C	ΔT_S	ΔT_N
E-H	Cr ₁ 94.82 Cr ₂ 109.63 SmC 175.98 N 219.17 I	66.35	43.19
E-OH	Cr 103.23 N 217.41 I	-	114.18
E-3Cl	Cr 80.81 N 160.89 I	-	87.08
E-2Cl	Cr 77.92 N 160.00 I	-	80.77
E-CH ₃	Cr 89.13 N 165.83 I	-	76.71
E-F	Cr 80.3 SmC 154.44 N 203.33 I	74.17	48.89

ΔT_N = thermal range of nematic phase, ΔT_S = thermal range of smectic phase.

2.2.4 Influence of Linking Group on Mesomorphic Properties

Usually, linking groups are used to extend the length and polarisability anisotropy of the molecular core in order to enhance the mesophase stability by more than any increase in melting point, producing wider mesophase ranges. The azo (-N=N-) and imine (-CH=N-) linking groups were among the early examples. These linking groups are used to connect aromatic core units and the conjugation is extended over the longer molecule which enhances the polarisability anisotropy (Collings and Hird, 1998b).

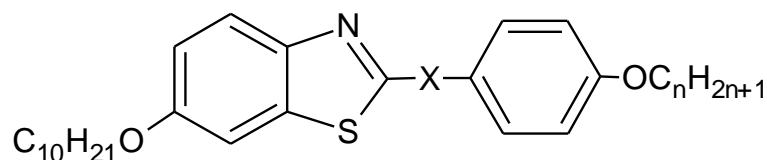
Three series of benzothiazole derivatives showing a typical rod-like geometry and incorporating three different linkage groups within the central core: imine-derivatives, 6-n-decyloxy-2-(4-alkoxybenzylidenamino)benzothiazoles (series A), amide-derivatives, N-[2-(6-n-decyloxybenzothiazolyl)]-4-n-alkoxy benzamides (series B), and azo-derivatives, 6-n-decyloxy-2-(4-n-alkoxyphenylazo) benzothiazoles (series C) with a general structure shown in Table 2.3 were reported by Belmer *et al.* (1999) to study the influence of the linking group on the mesomorphic properties.

Compounds in series A and series C show a very similar mesomorphic behaviour in terms of transition temperatures and mesophase type. Both displays nematic and smectic C mesomorphism. The nematic mesophase is observed for the entire range of n studied. This information suggests that similar

molecular interactions occur in both the series, giving rise to the same type of molecular arrangement and thermal stability. The members in both series with short alkyloxy chains ($n = 3-6$) exhibit nematic phase. A lateral interaction which is required for smectic phase is not favoured because of the difference of the volume occupied by the fixed C_{10} alkyloxy chains at one end of the molecule, and only a short range positional order can be achieved. However, as the length of both alkyloxy chains becomes similar ($n = 7-10$), the tilted smectic order is favoured.

Compounds in series B show a different mesomorphic behaviour. No mesophase is observed for the members with a short terminal chain ($n = 3-5$). The compound with $n = 6$ shows a monotropic nematic mesophase which then becomes enantiotropic for compounds with $n > 7$ onwards and they possess a higher melting point compared with their homologues in series A and B. Compounds with $n = 7-10$ show a smectic C mesophase. Such mesomorphic behaviour occurs due to the formation of hydrogen bonding between molecules which gives rise to a parallel molecular arrangement and hence promotes smectic mesomorphism by providing additional lateral intermolecular attraction and by lining up molecules in a layered order. However, the existence of hydrogen bonding between molecules inhibits the formation of nematic phase (Schroeder and Schroeder, 1976).

Table 2.3: Transition temperature and associated enthalpy changes of series A, B and C (Belmar *et al.*, 1999)



Series A X = N=CH (Imine)

Series B X = NHCO (Amide)

Series C X = N=N (Azo)

Compound	n	Transition temperature, °C
A3	3	Cr ₁ 75.0 Cr ₂ 79.9 N 103.2 I
A4	4	Cr 85.0 N 118.9 I
A5	5	Cr 75.9 N 112.2 I
A6	6	Cr 82.7 SmC 88.9 N 121.1 I
A7	7	Cr 80.8 SmC 101.2 N 120.3 I
A8	8	Cr 82.6 SmC 112.1 N 123.0 I
A9	9	Cr 80.8 SmC 116.4 N 121.7 I
A10	10	Cr 81.3 SmC 121.6 N 122.7 I
B3	3	Cr ₁ 72.4 Cr ₂ 100.6 Cr ₃ 104.8 Cr ₄ 112.6 I
B4	4	Cr ₁ 119.3 Cr ₂ 128.4 Cr ₃ 138.6 I
B5	5	Cr ₁ 80.9 Cr ₂ 134.8 I
B6	6	Cr ₁ 104.7 Cr ₂ 124.4 N 121.0 ^a I
B7	7	Cr ₁ 83.9 Cr ₂ 104.9 SmC 137.4 I
B8	8	Cr ₁ 88.0 Cr ₂ 100.5 SmC 132.8 I
B9	9	Cr ₁ 73.5 Cr ₂ 86.2 Cr ₃ 101.6 SmC 135.1 I
B10	10	Cr ₁ 100.6 Cr ₂ 116.0 SmC 124.5 N 127.5 I
C3	3	Cr 80.8 N 112.7 I
C4	4	Cr 83.8 N 121.9 I
C5	5	Cr 62.3 N 115.4 I
C6	6	Cr ₁ 65.4 Cr ₂ 48.3 SmC 75.2 N 121.7 I
C7	7	Cr 74.4 SmC 79.5 N 121.2 I
C8	8	Cr 70.7 SmC 95.0 N 123.8 I
C9	9	Cr 74.5 SmC 116.2 N 123.3 I
C10	10	Cr ₁ 56.0 Cr ₂ 77.9 SmC 114.7 N 123.1 I

^a indicates monotropic phase

CHAPTER 3
MATERIALS AND METHODS

3.1 Chemicals

All commercially available chemicals listed in Table 3.1 were used as received without further purification.

Table 3.1: List of chemicals used in this project

Chemical	Company
<ul style="list-style-type: none">• 4-Aminophenol• N, N'-dicyclohexylcarbodiimide (DCC)• 4-Dimethylaminopyridine (DMAP)• Hexanoic acid• Octanoic acid• Decanoic acid• Docecanoic acid• Tetradecanoic acid• Hexadecanoic acid• Octadecanoic acid• Deuterated chloroform• Ethyl acetate• TLC aluminum sheet silica gel 60 F₂₅₄	Merck (Germany)
<ul style="list-style-type: none">• 4-Dimethylaminobenzaldehyde• Dimethylformamide (DMF)	BDH Chemicals Ltd (England)
<ul style="list-style-type: none">• Absolute ethanol	John Kollin Corporation (UK)
<ul style="list-style-type: none">• Potassium bromide	Fisher Scientific (UK)
<ul style="list-style-type: none">• Chloroform• Dichloromethane (DCM)	R&M Chemicals (UK)

3.2 Synthesis

The synthetic scheme of 4-(dimethylaminobenzylidene)-4'-alkanoyloxy-anilines, **nDMABAA** is shown in Figure 3.1.

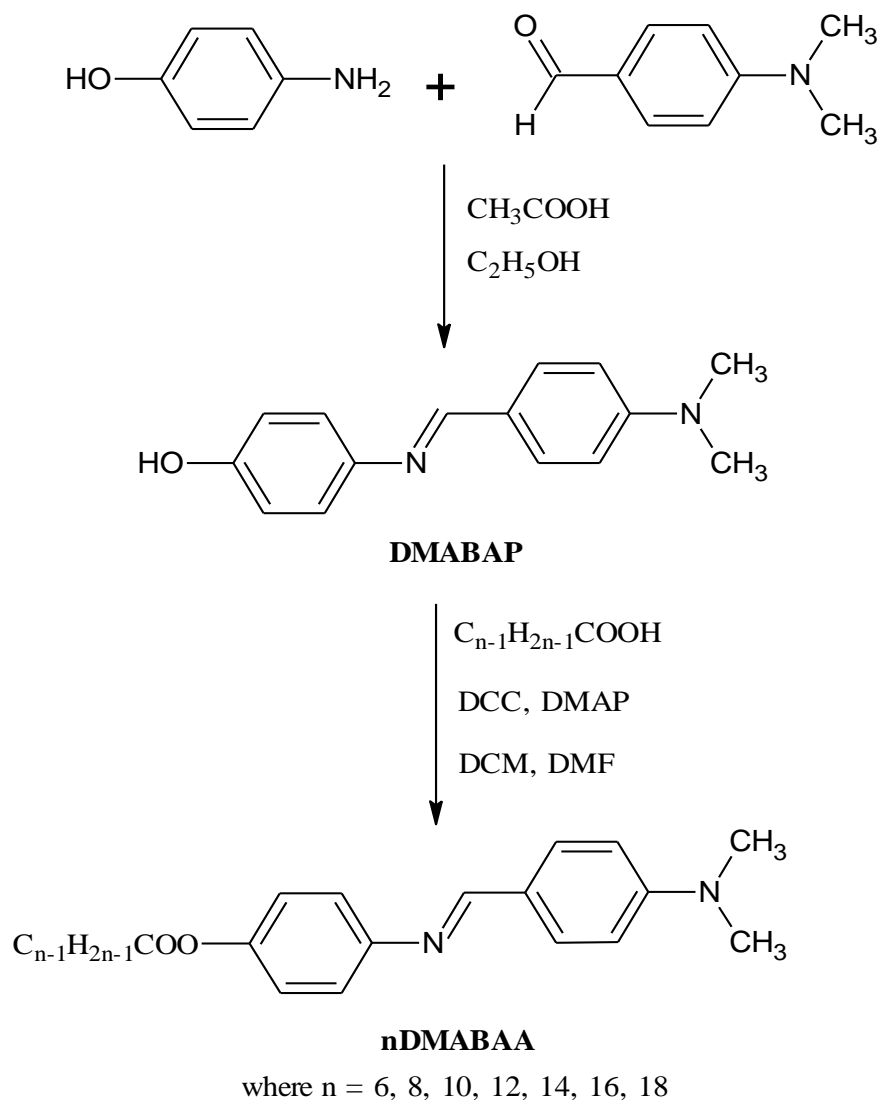


Figure 3.1: Synthetic scheme of 4-(dimethylamino)benzylidene-4'-alkanoyloxyanilines, nDMABAA

3.2.1 Synthesis of 4-{(4-(Dimethylamino)benzylidene)amino}phenol, DMABAP

A solution of 4-dimethylaminobenzaldehyde (0.45 g, 3.0 mmol) and 4-aminophenol (0.33 g, 3.0 mmol) in absolute ethanol (40 mL) was stirred for three hours in the presence of acetic acid (two drops). The yellowish Schiff base intermediate formed was collected by filtration through Buchner funnel, recrystallised using ethanol and dried in oven with 70% yield.

3.2.2 Synthesis of 4-(Dimethylamino)benzylidene-4'-alkanoyloxyanilines, nDMABAA

3.2.2.1 Synthesis of 4-(Dimethylamino)benzylidene-4'-hexanoyloxyaniline, 6DMABAA

Schiff base intermediate DMABAP (0.24 g, 1 mmol), hexanoic acid (0.12 g, 1 mmol) and DMAP (0.06 g, 0.5 mmol) were dissolved in a mixture of DCM and DMF (40 mL) with the ratio of 7:1 and stirred in an ice-bath. DCC (0.21 g, 1 mmol) dissolved in DCM (10 mL) was added to the solution dropwise upon stirring in the ice bath for an hour. The mixture solution was then continued stirring at room temperature overnight to ensure complete reaction. The reaction mixture was then filtered and the excess solvent was removed from the filtrate by evaporation at room temperature. The yellow solid obtained was recrystallised several times using ethanol to purify it. The final product was dried in oven. The percentage yield is 24.80 %.

3.2.2.2 Synthesis of 4-(Dimethylamino)benzylidene-4'-octanoyloxyaniline, 8DMABAA

The same procedures in synthesizing **6DMABAA** were repeated except that hexanoic acid was replaced by octanoic acid (0.14 g, 1 mmol). The percentage yield is 27.38 %.

3.2.2.3 Synthesis of 4-(Dimethylamino)benzylidene-4'-decanoyloxyaniline, 10DMABAA

The same procedures in synthesizing **6DMABAA** were repeated except that hexanoic acid was replaced by decanoic acid (0.17 g, 1 mmol). The percentage yield is 27.95 %.

3.2.2.4 Synthesis of 4-(Dimethylamino)benzylidene-4'-dodecanoyloxyaniline, 12DMABAA

The same procedures in synthesizing **6DMABAA** were repeated except that hexanoic acid was replaced by dodecanoic acid (0.20 g, 1 mmol). The percentage yield is 28.48 %.

3.2.2.5 Synthesis of 4-(Dimethylamino)benzylidene-4'-tetradecanoyloxy-aniline, 14DMABAA

The same procedures in synthesizing **6DMABAA** were repeated except that hexanoic acid was replaced by tetradecanoic acid (0.23 g, 1 mmol). The percentage yield is 37.33 %.

3.2.2.6 Synthesis of 4-(Dimethylamino)benzylidene-4'-hexadecanoyloxy-aniline, 16DMABAA

The same procedures in synthesizing **6DMABAA** were repeated except that hexanoic acid was replaced by hexadecanoic acid (0.26 g, 1 mmol). The percentage yield is 29.21 %.

3.2.2.7 Synthesis of 4-(Dimethylamino)benzylidene-4'-octadecanoyloxy-aniline, 18DMABAA

The same procedures in synthesizing **6DMABAA** were repeated except that hexanoic acid was replaced by octadecanoic acid (0.28 g, 1 mmol). The percentage yield is 32.40 %.

3.3 Characterisation

3.3.1 Thin Layer Chromatography (TLC)

This technique was used to determine the purity of the compounds. Mixture solvent of ethyl acetate and chloroform with the ratio of 1:1 was prepared as the mobile phase in a 50 mL beaker which was lined with a folded piece of filter paper to create a uniform and saturated atmosphere of solvent vapour. Appropriate amount of sample was dissolved in chloroform and a small spot of the resultant solution was applied onto the surface of an aluminum-backed silica gel plate (Merck 60 F₂₅₄), about 1.5 cm from the bottom edge. The TLC plate was then placed into the beaker to allow the solvent to move up until 0.5 cm from the top edge. After that, the TLC plate was removed and examined under short wave UV light. The existence of only one spot on the TLC plate indicates that the compound is pure.

3.3.2 Infrared Spectroscopy Analysis

Infrared (IR) spectra of **nDMABAA** series were recorded using a Perkin Elmer 2000 FT-IR spectrometer via KBr disc procedure in the frequency of 4000-400 cm⁻¹. First, small amount of sample and potassium bromide with the ratio of 1:10 were thoroughly ground in a mortar. Then, the sample-potassium bromide mixture was transferred into the cylinder bore, with the smooth surface of the lower pellet facing it. The upper pellet (smooth side down) was then inserted into

the bore, followed by the ram. The whole die assembly was placed in the hydraulic press and 4000 psi was exerted on it for about two minutes before removing it. The upper and lower die sections were separated. The pressed KBr disc was transferred to an appropriate disk holder and placed into the single beam spectrometer for IR analysis. All the significant bands were labeled and any appropriate notations (e.g., name, date, product etc) were added.

3.3.3 ^1H and ^{13}C Nuclear Magnetic Resonance Spectroscopy Analysis

^1H and ^{13}C NMR spectra were recorded using a Bruker Avance 300MHz UltrashieldTM NMR spectrometer. About 5 to 25 mg of sample was dissolved in CDCl_3 solvent at room temperature. Tetramethylsilane (TMS) was used as the internal standard. **14DMABAA** was chosen as the representative compound to be analysed for the ^1H NMR spectrum in the chemical shift range of 0.0-15.0 ppm and the ^{13}C NMR spectrum in the chemical shift range of 0.0-200.0 ppm.

3.3.4 Mass Spectrometry Analysis

Electron-ionisation mass spectrometry (EIMS) spectrum was recorded using Finnigan MAT95XL-T spectrometer, with ionisation electron impact in gas phase. The 70eV electron energy is used with 200 °C of source temperature. **14DMABAA** was chosen as the representative compound to be analysed.

3.3.5 Polarising Optical Microscopy (POM) Analysis

A Carl Zeiss polarising optical microscope equipped with a Linkam heating stage was used for temperature dependent studies of the liquid crystal textures. First, appropriate amount of sample was transferred onto the microscope slide and covered it with glass cover. The slide was then placed inside the hot stage. The focus of the microscope was adjusted to obtain a clear image of the sample. The heating and cooling rates were set accordingly to various samples. The heating or cooling process can be stopped at specific temperature when the mesophase transition happened to capture the image of the phase or even to record the whole mesophase transition process into video clips using computer. Phase identification was made by comparing the observed textures with those reported in the literature.

3.3.6 Differential Scanning Calorimetry (DSC) Analysis

Phase transition temperatures as well as enthalpy changes of the **nDMABAA** series were measured using a differential scanning calorimeter Mettler Toledo DSC823. About 1 mg to 2 mg of sample was weighed and transferred into a 45 μL crucible. The crucible was then sealed tightly with cover using sealing press and placed into the DSC chamber to start the scanning process. The cooling and heating process was run under 1 mL min^{-1} nitrogen flow with the rates and temperature ranges set accordingly for various samples.

CHAPTER 4
RESULTS AND DISCUSSION

4.1 Synthesis and Characterization of 4-{4-(Dimethylamino)benzylidene)amino}phenol, DMABAP

4.1.1 Synthesis Route of 4-{4-(Dimethylamino)benzylidene)amino}phenol, DMABAP

The Schiff base reaction occurs between an aromatic amine (4-aminophenol) and a carbonyl compound (4-dimethylaminobenzaldehyde) with ethanol as solvent and acetic acid as catalyst to fasten the rate of reaction. The synthesis route of Schiff base intermediate, **DMABAP** is shown in Figure 4.1.

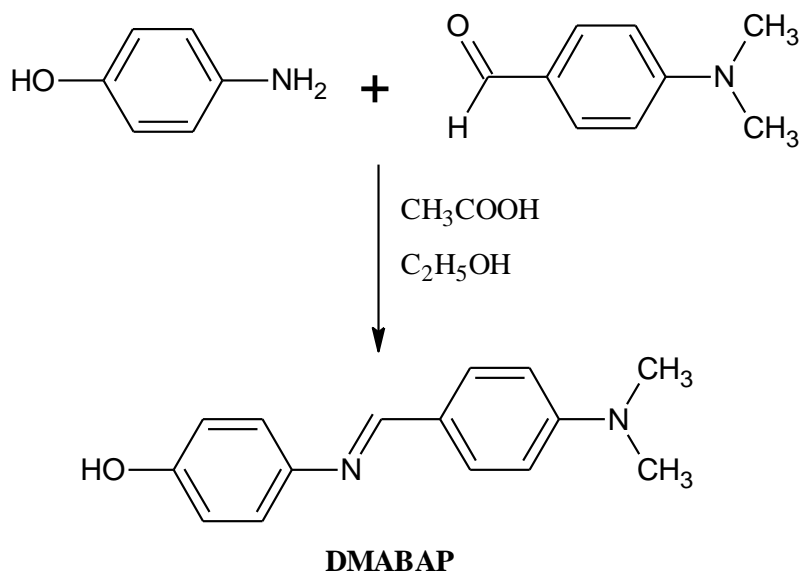


Figure 4.1: Synthesis route of Schiff base formation for DMABAP

4.1.2 Mechanism of Schiff Base Formation of DMABAP

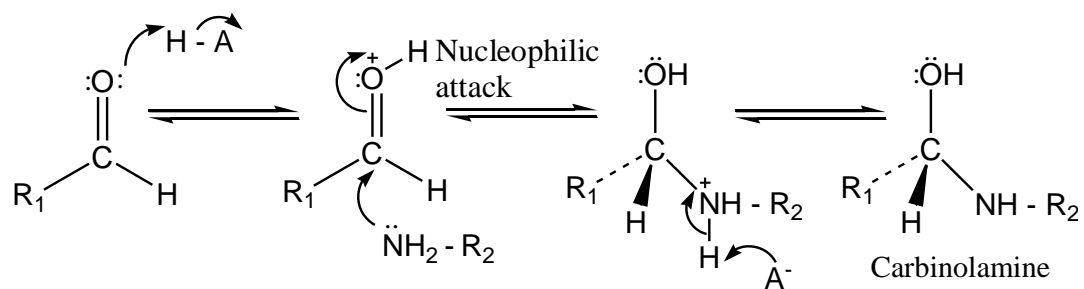
As illustrated in Figure 4.2, mechanism of Schiff base formation for **DMABAP** is divided into two parts: acid-catalyzed nucleophilic addition of amine to the carbonyl group (part I) and acid-catalyzed dehydration of carbinolamine (part II).

In part I, the mechanism begins with the H^+ ion from acetic acid forming a bond with the carbonyl oxygen atom, giving it a positive charge. The electrons which form this bond can be envisioned as coming from the carbonyl π bond, which leaves a positive charge on what was the carbonyl carbon. Once the π bond have been broken apart by forming a new bond to the hydrogen, the fairly weak nucleophile 1° amine, 4-aminophenol can then use its unshared electron pair on the nitrogen atom to form a new bond to the former carbonyl. For a weak nucleophile, an acid catalyst is needed so that the carbonyl carbon is prepared to share a pair of electrons as a new covalent bond; the unshared pair of electrons on an amine nitrogen is not nucleophilic enough to push the carbonyl π electrons away without help from an H^+ which breaks that π bond in an earlier step. However, the reaction stops if the amount of acid added is too much because amine which is a base will react with acid to form an ammonium ion. For each molecule of amine reacts with the molecule of acetic acid, the unshared electron pair has been used to make the N-H bond and is not available to act as a nucleophile to react with the carbonyl compound. Finally, the unstable

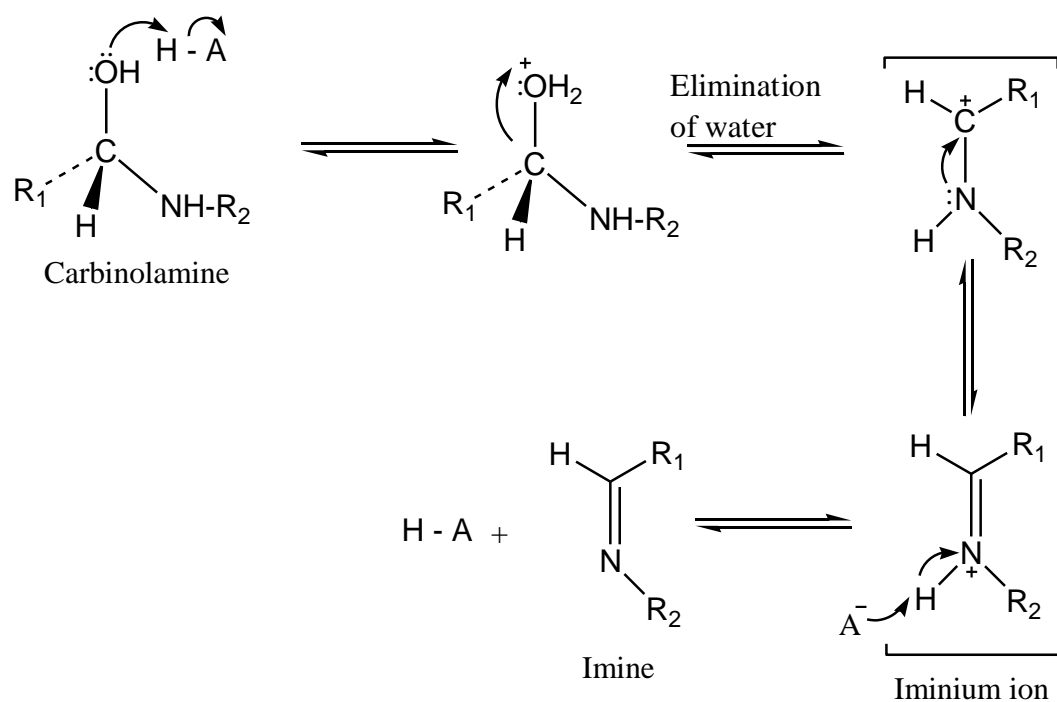
carbinolamine was formed through losing an H^+ ion, eliminating the positive charge on the amine nitrogen atom (McMichael, 2001).

In part II, the H^+ ion from acetic acid bonds to the carbonyl oxygen atom again and forms a H_2O group with a positively charged oxygen atom. The C-O bond then breaks apart to eliminate the H_2O group, leaving the carbon atom positively charged. The structure rearranges to form iminium ion by forming C=N bond using the unshared electron pair from amine nitrogen atom, eliminating the positive charge on carbon atom but leaving the amine nitrogen atom positively charged. Finally, the imine is formed by losing an H^+ ion, which also helps to balance the ions by replacing the used H^+ ion (Solomons and Fryhle, 2000).

Part I: Acid-catalyzed nucleophilic addition of amine to the carbonyl group



Part II: Acid-catalyzed dehydration of carbinolamine



where

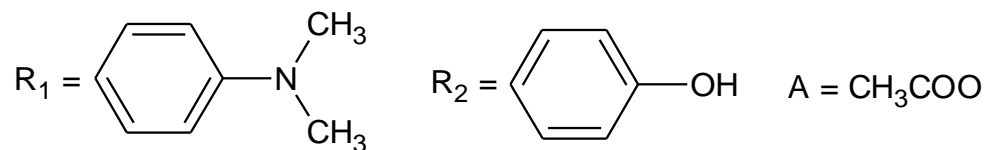


Figure 4.2: Mechanism of Schiff base formation for DMABAP

4.1.3 Infrared Spectral Analysis of Starting Materials and Intermediate Compound, DMABAP

The IR spectra for **DMABAP**, 4-dimethylaminobenzaldehyde and 4-aminophenol were shown in Figure 4.3 and their summarized infrared spectral data were shown in Table 4.1.

The IR spectrum of 4-aminophenol shows two sharp peaks at 3341 cm^{-1} and 3282 cm^{-1} which indicate the presence of N-H bond. Two N-H stretching absorption bands have confirmed that 4-aminophenol is primary amine; the higher-frequency band is due to the asymmetric vibration while the lower-frequency band is due to the symmetric vibration. There is a broad peak at the range of $3200\text{-}3550\text{ cm}^{-1}$ due to O-H bond but not obvious because it overlapped with the N-H peaks. A medium peak at 1615 cm^{-1} is due to N-H bending. The appearance of two strong peaks at 1510 and 1475 cm^{-1} indicates the presence of aromatic C=C bond. Strong peaks at 1256 and 1238 cm^{-1} can be ascribed to the presence of C-N bond and C-O bond respectively. Lastly, two out-of-plane C-H bending peaks at 845 cm^{-1} and 825 cm^{-1} indicates that the benzene ring is *para*-substituted.

In the IR spectrum of 4-dimethylaminobenzaldehyde, three weak peaks appeared at 2903 , 2795 and 2713 cm^{-1} . These peaks are typical C-H stretching for aldehyde compound. The C=O stretching peak is observed at 1661 cm^{-1} . Whereas,

two aromatic C=C stretching peaks are observed at 1594 and 1548 cm^{-1} , respectively. A strong peak appeared at 1370 cm^{-1} indicates the presence of methyl C-H symmetric bending. Two C-N stretching peaks have been detected: one at 1232 cm^{-1} due to aromatic C-N stretching while the other at 1163 cm^{-1} due to aliphatic C-N stretching. It is confirmed that the benzene ring is *para*-substituted since two peaks are observed at 825 and 812 cm^{-1} .

The IR spectrum of Schiff base intermediate, **DMABAP** shows a weak and broad O-H stretching peak at around 3437 cm^{-1} . There is also a weak absorption band at 2891 cm^{-1} which is most probably due to methyl C-H symmetric stretching. The strong absorption band emerged at 1609 cm^{-1} designates for C=N linking group. This value falls within the frequency range reported in the Schiff base compounds (Yeap *et al.*, 2006; Vora *et al.*, 2001). The peaks at 1590 and 1535 cm^{-1} can be ascribed to the presence of aromatic C=C bond. A strong peak emerged at 1374 cm^{-1} owns to the symmetric CH_3 bending. A strong aromatic C-N stretching peak is observed at 1276 cm^{-1} , having a higher frequency if compared to that of 4-aminophenol which appeared at 1256 cm^{-1} . This is due to the resonance effect that increases the double-bond character between the benzene rings and the attached nitrogen atom (Pavia *et al.*, 2009a). A medium peak emerged at 1241 cm^{-1} indicates the presence of C-O bond. The aliphatic C-N stretching peak also shifted to higher frequency if compared to that of 4-dimethylaminobenzaldehyde, emerging at 1182 cm^{-1} . In addition, the weak out-of-plane C-H bending peaks at 839 and 828 cm^{-1} proved that the benzene rings are attached with functional groups in the *para* position.

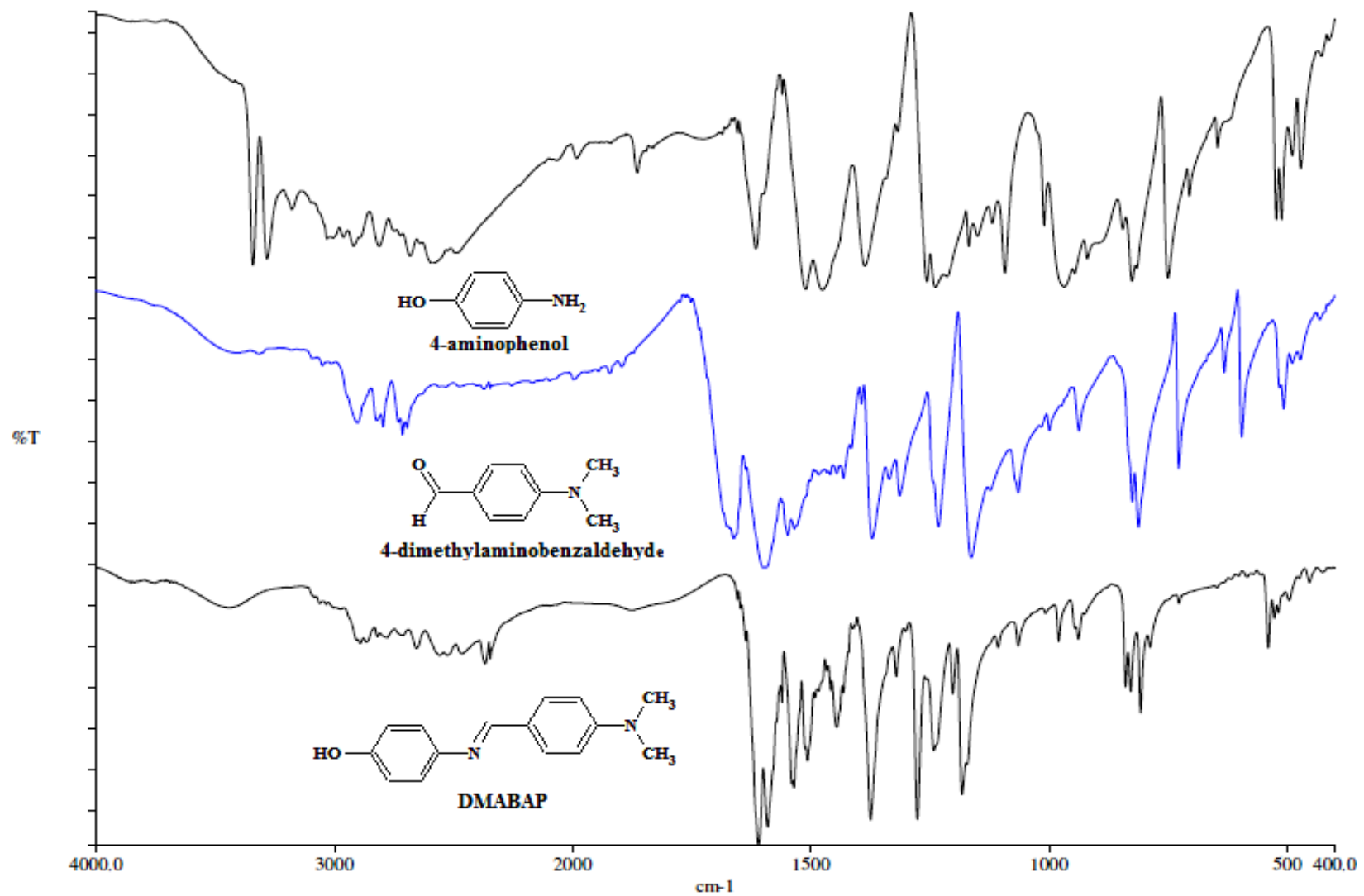


Figure 4.3 IR spectra of starting materials and intermediate compound, DMABAP

Table 4.1: IR spectral data of starting materials and intermediate compound, DMABAP

Compound	ν O-H	ν N-H	ν C-H _{ald}	ν _s CH ₃	ν C=O	δ N-H	ν C=C _{aro}	ν C=N	δ _s CH ₃	ν C-N	ν C-O	δ C-H _{oop}
4-aminophenol	-	3341s 3282s	-	-	-	1615m	1510s 1475s	-	-	1256s	1238s	845m 825s
4-dimethylamino benzaldehyde	-	-	2903w 2795w 2713w	-	1661m	-	1594s 1548m	-	1370m	1232m 1163s	-	825m 812s
DMABAP	3437w	-	-	2891w	-	-	1590s 1535m	1609s	1374s	1276s 1182m	1241m	839w 828w

w = weak, m = medium, s = strong, ν = stretching, δ = bending, s = symmetric, oop = out-of-plane, aro = aromatic, ald = aldehyde

4.2 Synthesis and Characterization of 4-(Dimethylamino)benzylidene-4'-alkanoxyanilines, **nDMABAA**

4.2.1 Synthesis Route of 4-(Dimethylamino)benzylidene-4'-alkanoxyaniline, **nDMABAA**

Steglich esterification occurred between the Schiff base intermediate, **DMABAP** and fatty acids with different number of carbon atom ($C_{n-1}H_{2n-1}COOH$, $n = 6, 8, 10, 12, 14, 16, 18$) with DCC as coupling reagent, DMAP as catalyst and DCM, DMF as solvents to form the ester compounds, **nDMABAA**. The synthesis route of Steglich esterification for **nDMABAA** is shown in Figure 4.4.

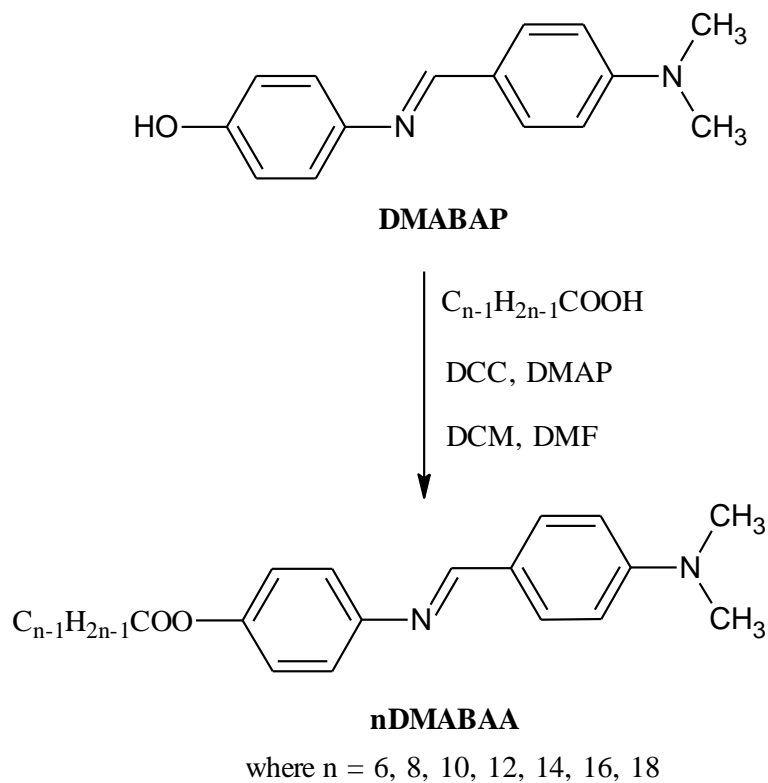


Figure 4.4: Synthesis route of Steglich esterification for **nDMABAA**

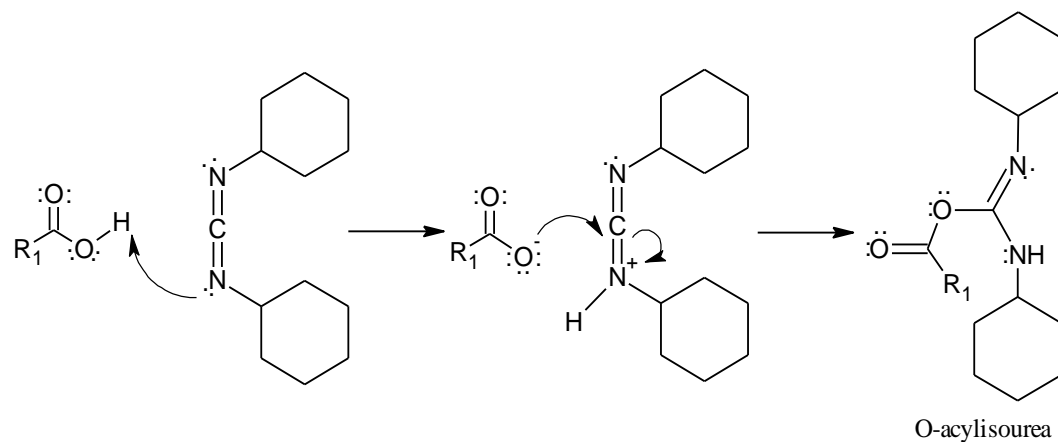
4.2.2 Mechanism of Steglich Esterification of nDMABAA

Mechanism of Steglich esterification for **nDMABAA** is illustrated in Figure 4.5. The mechanism is divided into two parts: formation of O-acylisourea intermediate (part I) and formation of DHU and the corresponding ester (part II).

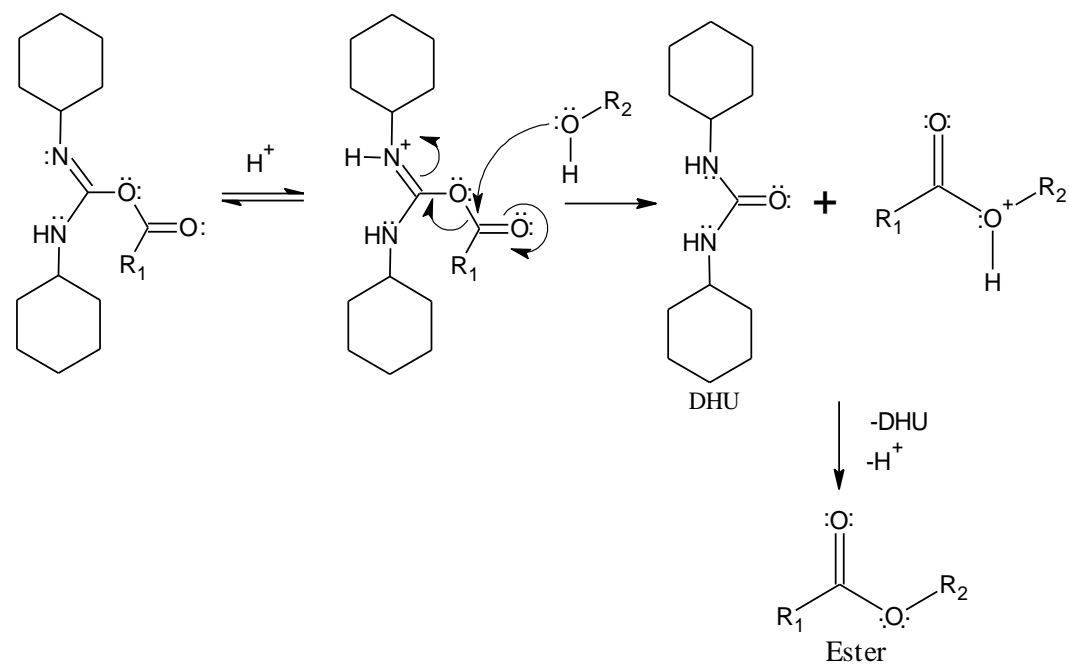
In part I, DCC first forms a bond to the hydrogen atom of fatty acid using the unshared electron pair on its nitrogen atom, giving the oxygen atom a negative charge and the nitrogen atom a positive charge. The negatively charged oxygen atom then attacks the carbon atom of DCC, breaking the π bond and eliminating the positive charge on the nitrogen atom to form the O-acylisourea intermediate, which offers reactivity similar to the corresponding fatty acid anhydride.

In part II, the mechanism starts with the H^+ ion forming a bond with the unshared electron pair on nitrogen atom, giving the nitrogen atom a positive charge. The **DMABAP** then attacks the carbonyl carbon atom with the unshared electron pair on its oxygen atom, breaking the C-O bond. The electrons from the breaking of C-O bond are transferred to eliminate the positive charge on the nitrogen atom, forming the undesired by-product DHU. Finally, the corresponding ester is formed by losing an H^+ ion, which also helps to balance the ions by replacing the used H^+ ion (Neises and Steglich 1978).

Part I: Formation of O-acylisourea intermediate



Part II: Formation of DHU and the corresponding ester



where

$R_1 = -C_5H_{11}, -C_7H_{15}, -C_9H_{19}, -C_{11}H_{23}, -C_{13}H_{27}, -C_{15}H_{31}, -C_{17}H_{35}$

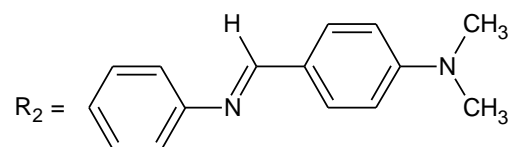
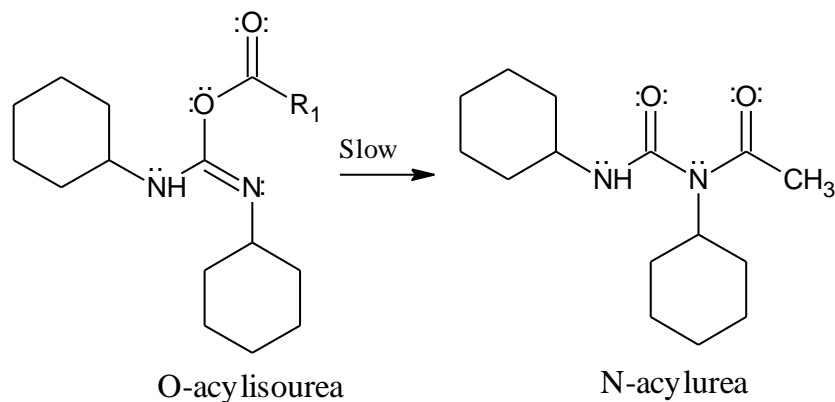


Figure 4.5: Mechanism of Steglich esterification for nDMABAA

If the esterification process is slow, a side-reaction occurs, diminishing the final yield or complicating purification of the product. As illustrated in Figure 4.6, this side-reaction is a 1,3-rearrangement of the O-acylisourea to an N-acylurea which is unable to further react with **DMABAP**.



where

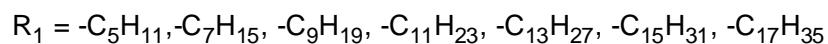


Figure 4.6: 1,3-Rearrangement of O-acylisourea to N-acylurea

To suppress this reaction, DMAP which is a stronger nucleophile than **DMABAP** is added. Its dimethylamino group acts as an electron-donor substituent, increasing both nucleophilicity and basicity of the pyridine nitrogen. DMAP reacts with the O-acylisourea to form a reactive amide (active ester). This intermediate cannot form intramolecular side products but reacts rapidly with **DMABAP**. In this way, the DMAP acts as an acyl transfer reagent and subsequent reaction with **DMABAP** forms the ester (Neises and Steglich, 1978). The reaction route is shown in Figure 4.7.

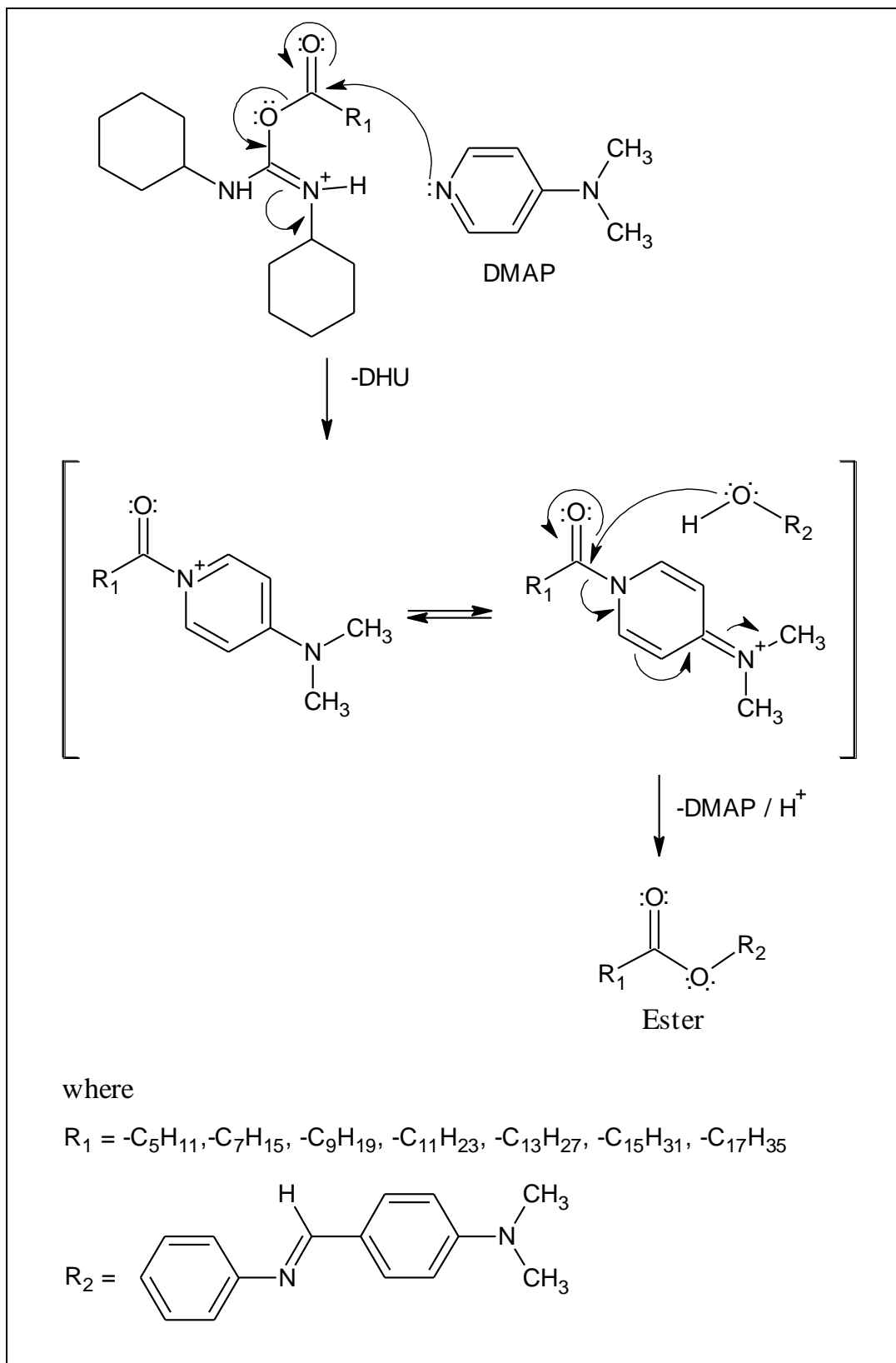


Figure 4.7: Reaction route of DMAP

4.2.3 Infrared Spectral Analysis of nDMABAA

16DMABAA is chosen as the representative compound for **nDMABAA** series to be discussed. The IR spectra for **16DMABAA**, palmitic acid and **DMABAP** were shown in Figure 4.8 and their summarized infrared spectral data were shown in Table 4.2. Besides that, the IR spectra for all members in **nDMABAA** series and their summarized infrared spectral data were also shown in Figure 4.9 and Table 4.3, respectively.

The IR spectrum of palmitic acid shows a weak and broad O-H stretching peak at around 3450 cm^{-1} . Two strong methylene C-H stretching peaks appeared at 2917 and 2849 cm^{-1} ; the higher-frequency peak is due to the asymmetric vibration while the lower-frequency peak is due to the symmetric vibration. A strong peak at 1701 cm^{-1} can be ascribed to C=O bond of the carboxylic acid. In addition, there is also a weak peak at 1295 cm^{-1} which is most probably due to the presence of C-O bond.

The IR spectrum of **16DMABAA** also shows two strong peaks at 2918 and 2850 cm^{-1} which indicate the presence of methylene C-H asymmetric and symmetric stretching. For those members in the series with shorter alkanoyloxy chain such as **6DMABAA** and **8DMABAA**, a weak methyl C-H asymmetric stretching emerges around 2950 cm^{-1} as the intensity of the methylene C-H asymmetric stretching peak is weaker, no longer overlapping it. A strong peak

appeared at 1752 cm^{-1} indicates that the -OH group of **DMABAP** had reacted with the -COOH group of palmitic acid to form the ester bond. This peak has been shifted to a higher frequency if compared to that of palmitic acid which appeared at 1701 cm^{-1} . This is because the single-bonded oxygen atom which is more electronegative than carbon atom tends to draw in the electrons between the carbon and oxygen atoms through its electron-withdrawing effect, so that the ester bond becomes somewhat stronger and thus resulting in a higher absorption frequency (Pavia *et al.*, 2009a). A medium peak appeared at 1590 cm^{-1} proved the presence of aromatic C=C bond in the compound. The C=N stretching peak and CH₃ bending peak appears at 1608 and 1368 cm^{-1} respectively, showing lower intensity if compared to that of the intermediate, **DMABAP**. Two C-O stretching peak are observed: the C-O stretch next to the carbonyl group (the “intermediate” side) of the ester is observed at 1207 cm^{-1} while the C-O stretch for the “fatty acid” part of the ester appears as a weaker band at 1193 cm^{-1} . The medium peaks emerged at 1179 and 1162 cm^{-1} are designated for C-N bond. It is usually hard to determine the C-O and C-N stretching peaks as both of them having similar range of absorption frequency which is around $1000\text{-}1300\text{ cm}^{-1}$. They tend to overlap each others, especially for those derivatives with shorter alkanoyloxy chain, **6DMABAA** and **8DMABAA**. Lastly, the strong peak emerged at 1142 cm^{-1} can be ascribed to -COO stretching. Whereas, the weak out-of-plane C-H bending peaks at 847 cm^{-1} and 817 cm^{-1} indicate that the benzene rings are *para*-substituted.

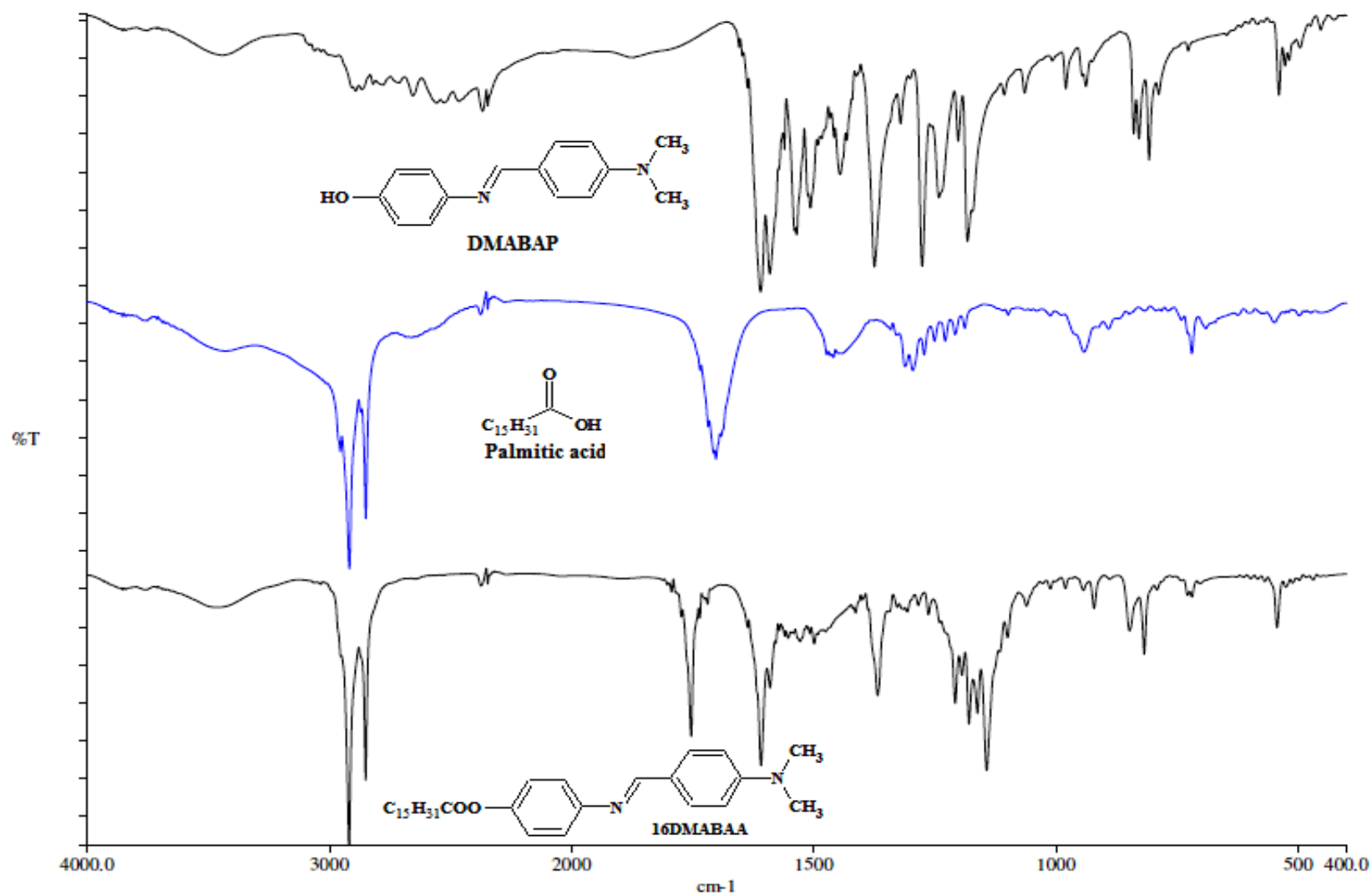


Figure 4.8: IR spectra of 4-dimethylaminobenzaldehyde, palmitic acid and 16DMABAA

Table 4.2: IR spectral data of 4-dimethylaminobenzaldehyde, palmitic acid and 16DMABAA

Compound	ν O-H	ν_{as} CH ₂ ν_s CH ₂	ν_s CH ₃	ν C=O	ν C=N	ν C=C _{aro}	δ CH ₃	ν C-N	ν C-O	ν COO	δ C-H _{oop}
DMABAP	3437w	-	2891w	-	1609s	1590s 1535m	1374s	1276s 1182m	1241m	-	839w 828w
Palmitic acid	3450w	2917s 2849s	-	1701s	-	-	-	-	1295w	-	-
16DMABAA	-	2918s 2850s	-	1752s	1608s	1590m	1368m	1179m 1162m	1207m 1193w	1142s	847w 817w

w = weak, m = medium, s = strong, ν = stretching, δ = bending, s = symmetric, as = asymmetric, oop = out-of-plane, aro = aromatic

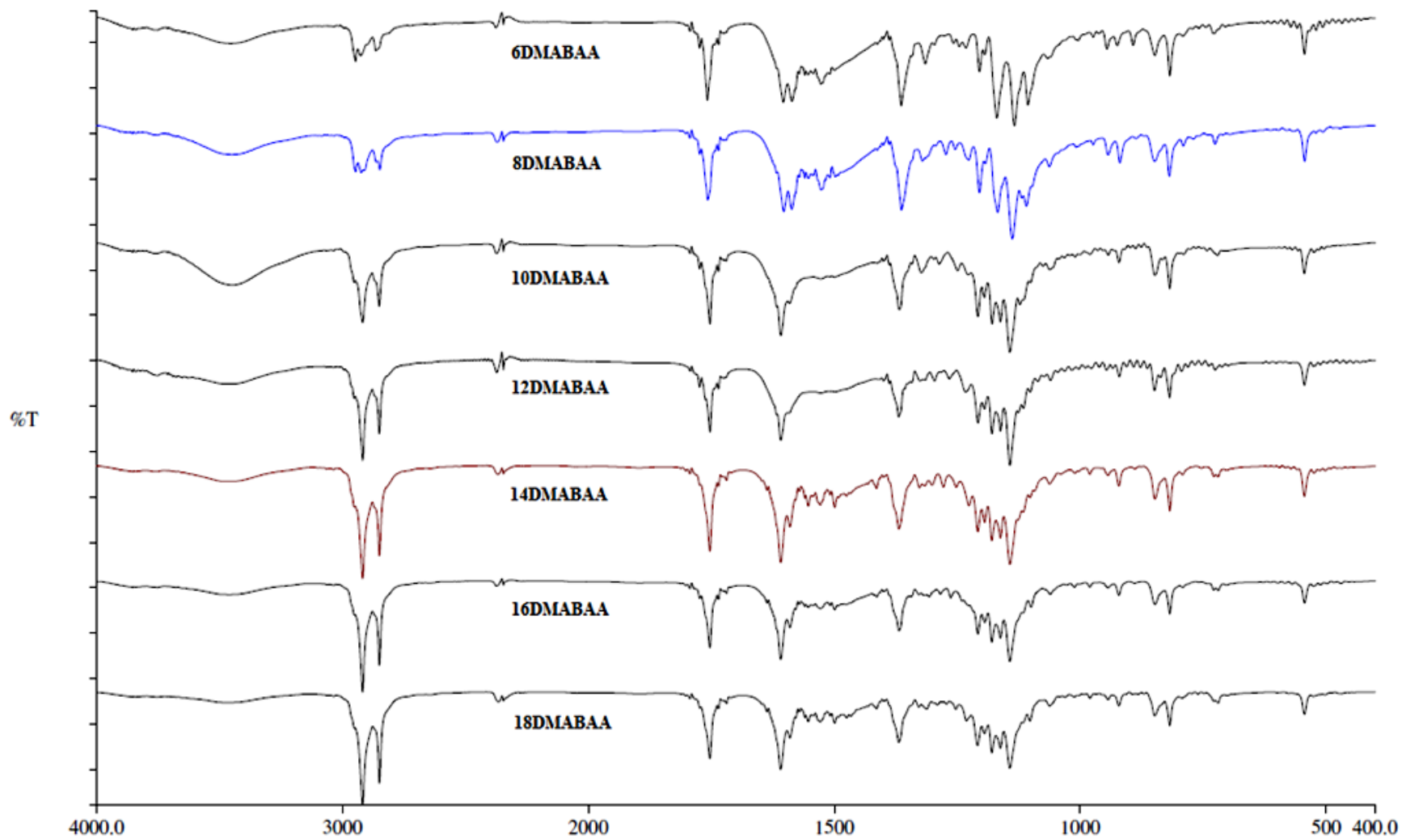


Figure 4.9: IR spectra of nDMABAA where n = 6, 8, 10, 12, 14, 16 and 18

Table 4.3: IR spectral data of nDMABAA where n = 6, 8, 10, 12, 14, 16 and 18

Compound	$\nu_{as} \text{CH}_3$	$\nu_{as} \text{CH}_2$ $\nu_s \text{CH}_2$	$\nu \text{C}=\text{O}$	$\nu \text{C}=\text{N}$	$\nu \text{C}=\text{C}_{\text{aro}}$	δCH_3	$\nu \text{C}-\text{N}$	$\nu \text{C}-\text{O}$	νCOO	$\delta \text{C}-\text{H}_{\text{oop}}$
6DMABAA	2947w	2926w 2864w	1757m	1603m	1585m	1363m	1167s	1204m 1193w	1133s	848w 817m
8DMABAA	2947w	2924w 2848w	1757m	1602m	1586m	1363m	1167m	1204m 1192w	1137s	848w 818m
10DMABAA	-	2918s 2850m	1752s	1608s	1590m	1367m	1178m 1162m	1207m 1194w	1142s	847w 817w
12DMABAA	-	2917s 2850s	1752s	1608s	1591m	1368m	1179m 1161m	1207m 1194w	1142s	848w 818w
14DMABAA	-	2918s 2850s	1752s	1608s	1590m	1368m	1179m 1162m	1208m 1194w	1142s	847w 817w
16DMABAA	-	2918s 2850s	1752s	1608s	1590m	1368m	1179m 1162m	1207m 1193w	1142s	847w 817w
18DMABAA	-	2918s 2849s	1752s	1608s	1590m	1368m	1179m 1162m	1208m 1194w	1142s	848w 817w

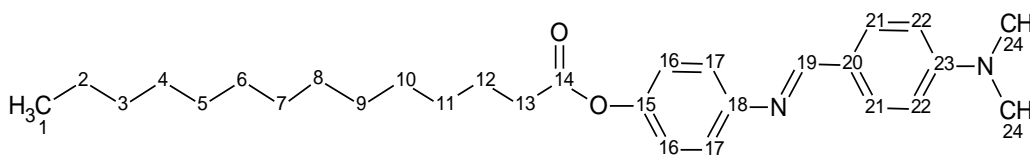
w = weak, m = medium, s = strong, ν = stretching, δ = bending, s = symmetric, as = asymmetric, oop = out-of-plane, aro = aromatic

4.2.4 Nuclear Magnetic Resonance Analysis

4.2.4.1 ¹H NMR Spectral Analysis of nDMABAA

14DMABAA is chosen as the representative for **nDMABAA** series to be discussed. The molecular structure of **14DMABAA** with the numbering and data are tabulated in Table 4.4 while its ¹H NMR spectrum is shown in Figure 4.10.

Table 4.4: ¹H NMR data and the proposed structure of 14DMABAA



Proton(s)	Number(s) of H	Coupling constant, J (Hz)	Chemical shift, ppm	Peak(s)
H1	3	-	0.88-0.92	t
H2-H11	20	-	1.25-1.45	m
H12	2	-	1.70-1.83	q
H13	2	-	2.55-2.60	t
H24	6	-	3.05-3.10	s
H22	2	8.93	6.72-6.80	d
H21	2	8.80	7.06-7.11	d
H17	2	8.79	7.20-7.25	d
H16	2	8.78	7.75-7.80	d
H19	1	-	8.33	s

TMS as internal standard, CDCl₃ as solvent, s = singlet, d = doublet, t = triplet, q = quintet, m = multiplet

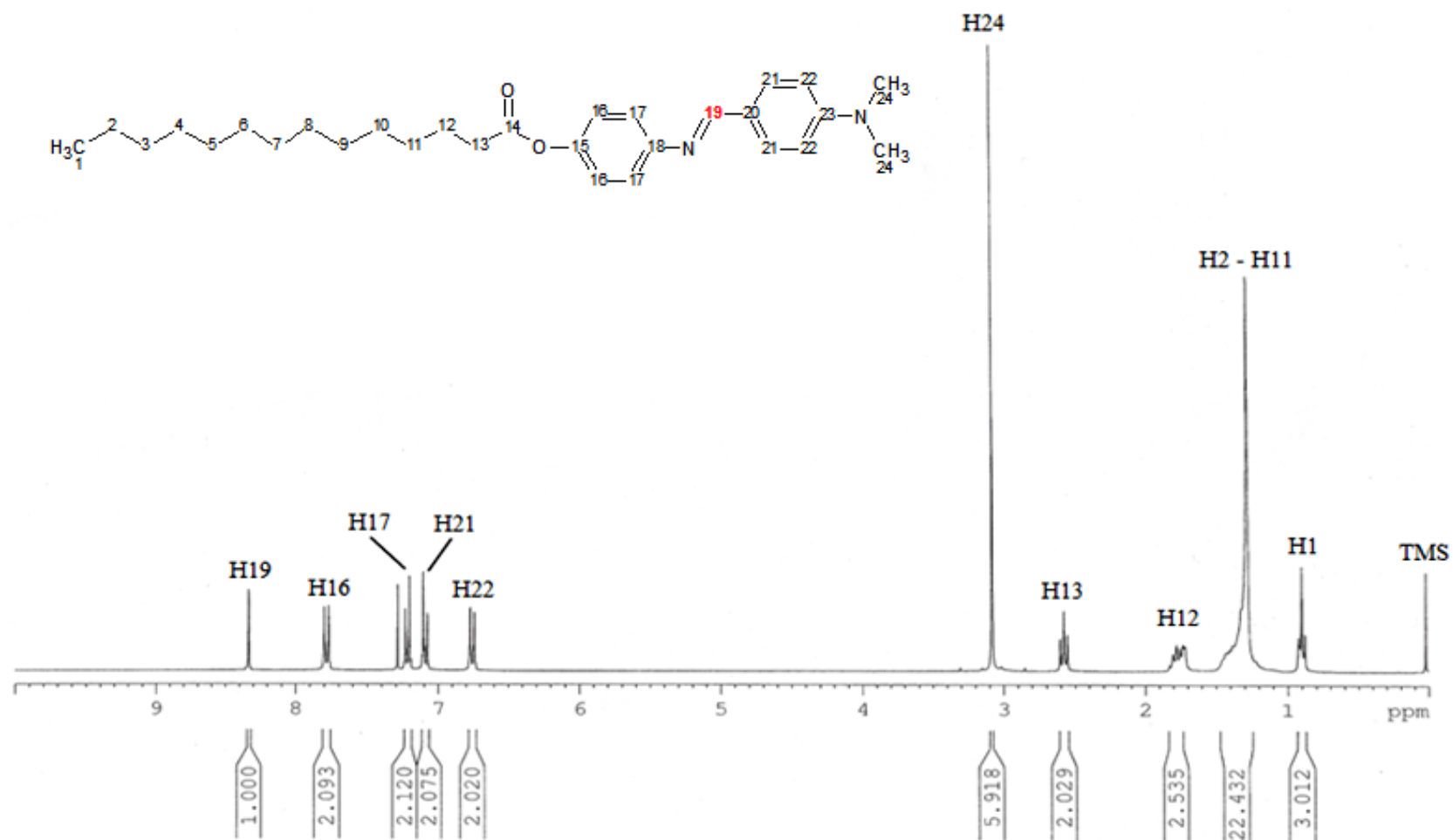


Figure 4.10: ¹H NMR spectrum of 14DMABAA

The most upfield triplet peak observed at $\delta = 0.88-0.92$ ppm is due to the presence of methyl protons (H1) at the end of the long alkyl chain. The chemical shift of multiplet peak at $\delta = 1.25-1.45$ ppm is attributed to the methylene protons (H2-H11) of long alkyl chain. A quintet peak at $\delta = 1.70-1.83$ ppm can be assigned to the methylene protons (H12) as it obeys the (n+1) rule perfectly; it has four equivalent neighbours (n=4) and is split into $n+1 = 5$ peaks (a quintet). Besides that, this peak has greater chemical shift than those previous methylene protons due to the deshielding effect of the anisotropic field of the carbonyl group (C=O). The same explanation also applies to the triplet peak at $\delta = 2.55-2.60$ ppm, the methylene protons (H13) which has two equivalent neighbours gives rise to a triplet peak, obeying the (n+1) rule. This peak has even greater chemical shift than the methylene protons (H12) as all its protons are on a carbon that is directly bonded to the carbonyl group, leading to a greater deshielding effect. The methyl protons (H24) α to the amino group are also slightly deshielded by the presence of the electron-withdrawing nitrogen atom, and they give rise to the most intense singlet peak at $\delta = 3.05-3.10$ ppm.

Four distinct doublet peaks at $\delta = 6.72-7.80$ ppm can be assigned to the eight aromatic protons (H16, H17, H21 and H22) as these protons are greatly deshielded by the large anisotropic field that is generated by the circulation of the aromatic π electrons. Besides this, electron-withdrawing nitrogen and oxygen atom attached to the rings also deshielded the attached protons further by withdrawing electron density from the ring through resonance interaction (Pavia

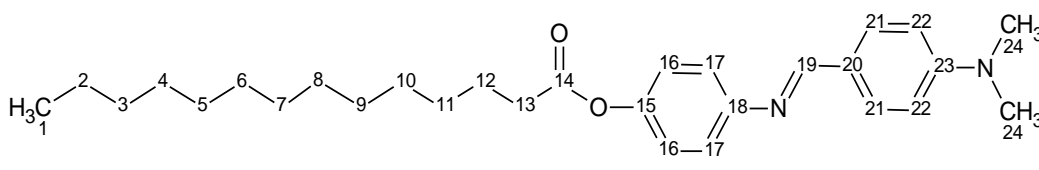
et al., 2009b). The doublet peaks shown at $\delta = 7.75-7.80$ and $7.20-7.25$ ppm are attributed to H16 and H17 aromatic protons respectively. H16 aromatic protons are more deshielded than H17 aromatic protons due to the greater electron-withdrawing effect of oxygen atoms in ester linking group than the nitrogen atom in imine linking group.

The deshielding effect of the electron-withdrawing nitrogen atom of the imine linking group on H21 aromatic protons are expected to be slightly weaker compared to H17 aromatic protons as they are more distant away, emerging as a doublet peak at $\delta = 7.06-7.11$ ppm. On the other hand, H22 aromatic protons are the least deshielded among all aromatic protons due to the presence of electron-donating group $-\text{N}(\text{CH}_3)_2$ which increases the shielding of these protons causing them to move upfield, emerging as a doublet peak at $\delta = 6.72-6.80$ ppm. All the eight aromatic protons have coupling constant, J close to 9 Hz which indicates that these protons are *ortho*-substituted to the rings. Lastly, the singlet peak observed at the most downfield region, $\delta = 8.33$ ppm is due to H19 proton of imine linking group which does not have any adjacent proton (Yeap *et al.*, 2006). This proton is greatly shifted downfield due to the sp^2 hybridisation effect of double bond, the electron-withdrawing effect of nitrogen atom and even the anisotropy effect of benzene ring.

4.2.4.2 ^{13}C NMR Spectral Analysis of nDMABAA

The molecular structures of nDMABAA series are further verified using ^{13}C NMR analysis technique. The molecular structure of the representative compound, 14DMABAA with the numbering and data are tabulated in Table 4.5 while its ^{13}C NMR spectrum is shown in Figure 4.11.

Table 4.5: ^{13}C NMR data and the proposed structure of 14DMABAA



Carbon(s)	Chemical shift, ppm
C1	14.6
C2	23.2
C3	25.5
C4-C11	29.6-30.2
C12	32.5
C13	35.0
C24	40.7
C22	112.0
C21	122.2
C17	122.5
C23	124.5
C16	130.9
C20	148.5
C18	151.0
C15	153.0
C19	161.0
C14	173.1

TMS as internal standard, CDCl_3 as solvent

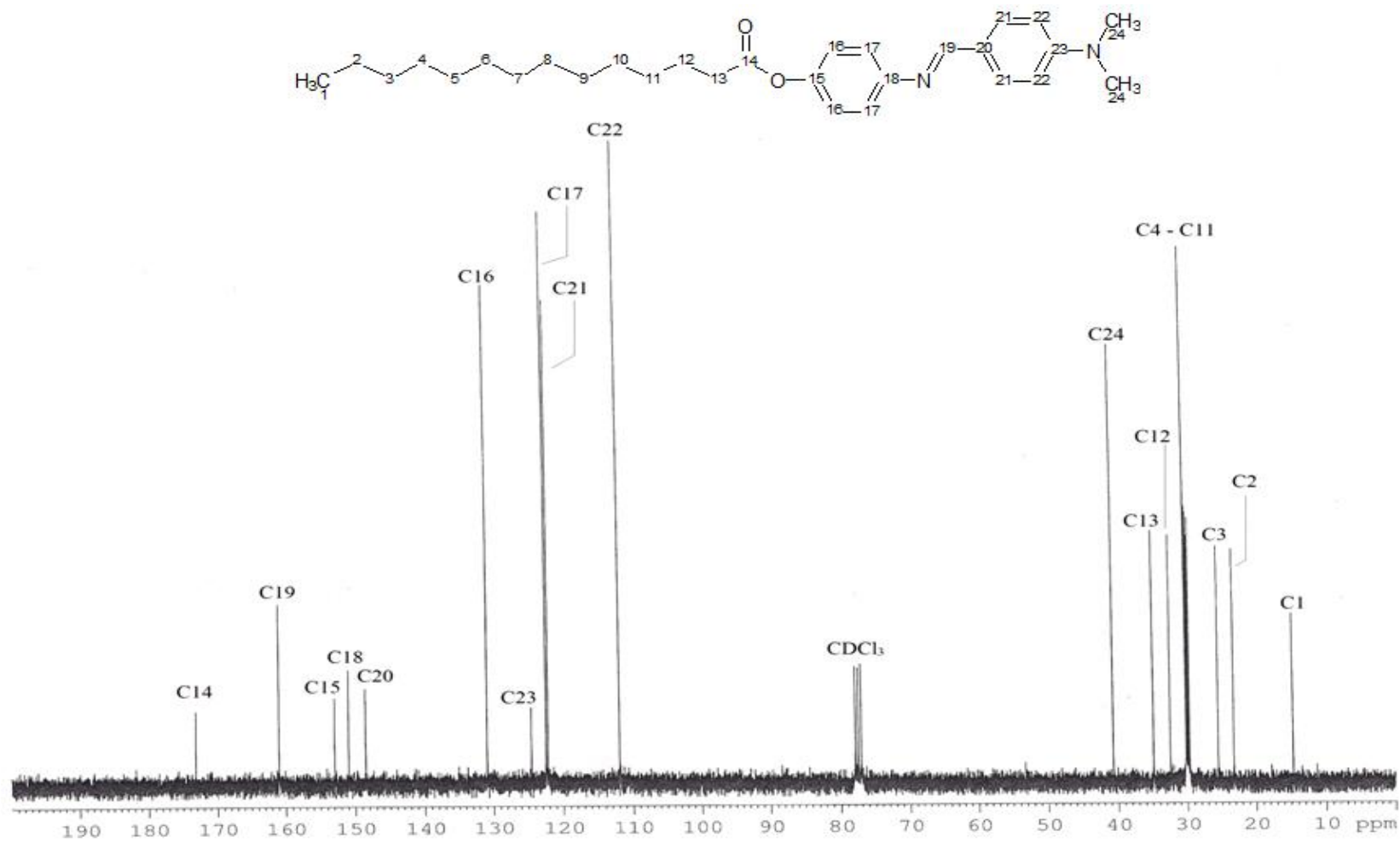


Figure 4.11: ^{13}C NMR spectrum of 14DMABAA

The most upfield peak observed at $\delta = 14.6$ ppm is attributed to C1 methyl carbon and peaks at $\delta = 23.1$ -35.0 ppm is contributed by the C2-C13 methylene carbons of long alkyl chain. The peak at 35.0 ppm is assigned to C13 carbon due to the electronegativity carbonyl oxygen which deshielded the carbon and shifted the peak to lower field region compared to the other methylene carbons. The deshielding effect diminishes with distance, C12 carbon which is one more carbon away from the oxygen atom than C13 carbon showed a peak at $\delta = 32.5$ ppm, shifted slightly upfield compared to that of C13 carbon. The peaks at $\delta = 23.2$, 25.5 and 29.6-30.2 ppm are assigned to C2, C3 and C4-C11 carbons, respectively. These peaks have high intensity because of the nuclear Overhauser enhancement (NOE) effect and the interaction of the spin-spin dipoles operates through space. The peaks at $\delta = 40.7$ ppm is ascribed to C24 methyl carbons as the electron-withdrawing nitrogen atom deshielded these carbons, causing them to move downfield. Again, the high intensity of the peak can be explained by the NOE effect on both of the two equivalent carbons. The three-peak pattern centered at $\delta = 77.5$ ppm is due to the solvent CDCl_3 . This pattern results from the coupling of a deuterium (^2H) nucleus to the ^{13}C nucleus (Pavia *et al.*, 2009b).

Peaks at $\delta = 112.0$ -153.0 ppm are assigned to the twelve aromatic carbons (C15-C18 and C20-C23). These carbons are greatly deshielded by the large anisotropic field that is generated by the circulation of the aromatic π electrons. Since C15, C18, C20 and C23 aromatic carbons are *ipso* carbon which is the one to which the substituent (except hydrogen) is directly attached, it can be expected

that they are having weaker peaks compared to *ortho* or *meta* C16, C17, C21 and C22 aromatic carbons due to weaker NOE effect. The intensities of C16, C17, C21 and C22 aromatic carbons are greatly enhanced by the NOE effect of the heteronuclear (carbon-hydrogen) interaction. Besides this, these *para* or *meta* aromatic carbons are equivalent by symmetry and that each gives only a single but high intensity peak.

The peaks emerged at $\delta = 153.0$ and 151.0 ppm are attributed to C15 and C18 aromatic carbons, respectively. C15 aromatic carbon is more deshielded compared to C18 aromatic carbon as it is directly attached to oxygen atom that has a greater electron-withdrawing effect than nitrogen atom. Besides this, the lone pair on the oxygen atom is delocalized by resonance, forming a partial double bond with the carbonyl carbon and thus further deshielding the carbon. Even though the C18 aromatic carbon is also affected by sp^2 hybridisation effect of the double bond in imine linking group, the deshielding effect is still expected to be lower than the deshielding effect caused by the two higher electron-withdrawing oxygen atoms and the resonance effect of carbonyl group. The same explanation also applies to C16 and C17 aromatic carbons, C16 aromatic carbons which are β to oxygen atom are more deshielded compared to C17 aromatic carbons which are β to nitrogen atom, emerging at $\delta = 130.9$ and 122.5 ppm, respectively. The deshielding effect of electron-withdrawing oxygen or nitrogen atom diminished with distance. This explains why the C15 and C18 aromatic carbons which are directly attached to the electron-withdrawing oxygen or

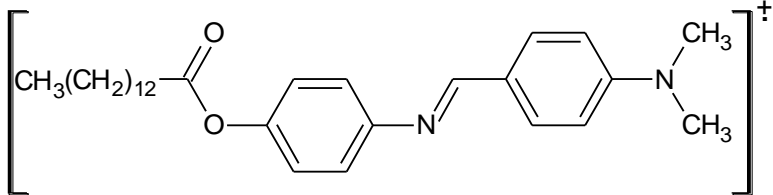
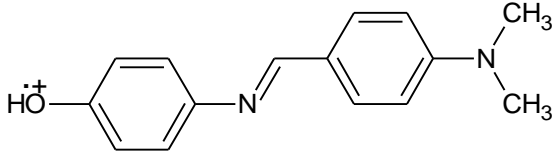
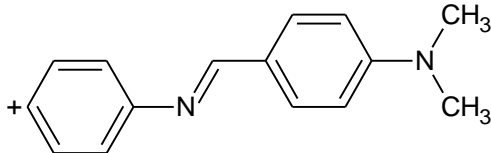
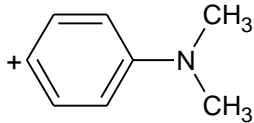
nitrogen atom are more deshielded than C16 and C17 aromatic carbons which are one carbon bond distance away. Due to the same reason, the C20 aromatic carbon which is not directly attached to any electron-withdrawing groups also expected to acquire weaker deshielding effect, emerging at $\delta = 148.5$ ppm. The deshielding effect becomes even weaker when approaching the C21 and C22 aromatic carbons which are more distant away from any electron-withdrawing groups. On the other hand, electron-donating group $-\text{N}(\text{CH}_3)_2$ tends to increase the shielding of carbons causing them to move upfield. This explains why C22 and C23 aromatic carbons are the least deshielded among all corresponding aromatic carbons, emerging at $\delta = 112.0$ and 124.5 ppm, respectively.

The peak appears at the most downfield region at $\delta = 173.1$ ppm is ascribed to the C14 carbon of carbonyl group ($\text{C}=\text{O}$). It has the largest chemical shifts due to both the sp^2 hybridisation effect and the fact that two electronegative oxygen atoms are directly attached the carbonyl carbon, deshielding it even further. Lastly, the peak at $\delta = 161.0$ ppm is due to the existence C19 azomethine carbon. It is greatly shifted downfield due to the sp^2 hybridisation effect of double bond, the electron-withdrawing effect of nitrogen atom and even the anisotropy effect of benzene ring (Pavia *et al.*, 2009b).

4.2.5 Mass Spectrometry Analysis of nDMABAA

The molecular structure of nDMABAA series are elucidated by using EI-mass spectrometry analysis technique. The m/z values and proposed fragments of the representative compound, 14DMABAA are tabulated in Table 4.6 while its EI-mass spectrum is shown in Figure 4.12.

Table 4.6: m/z value and the proposed fragment of 14DMABAA

m/z	Proposed fragment
450.4 (M ⁺)	
240.2 (base peak)	
223.2	
211.0	$\text{CH}_3(\text{CH}_2)_{12}-\overset{+}{\text{C}}=\text{O} \longleftrightarrow \text{CH}_3(\text{CH}_2)_{12}-\text{C}\equiv\overset{+}{\text{O}}$
120.1	
57.1	$\text{CH}_3(\text{CH}_2)_3^+$
43.1	$\text{CH}_3(\text{CH}_2)_2^+$

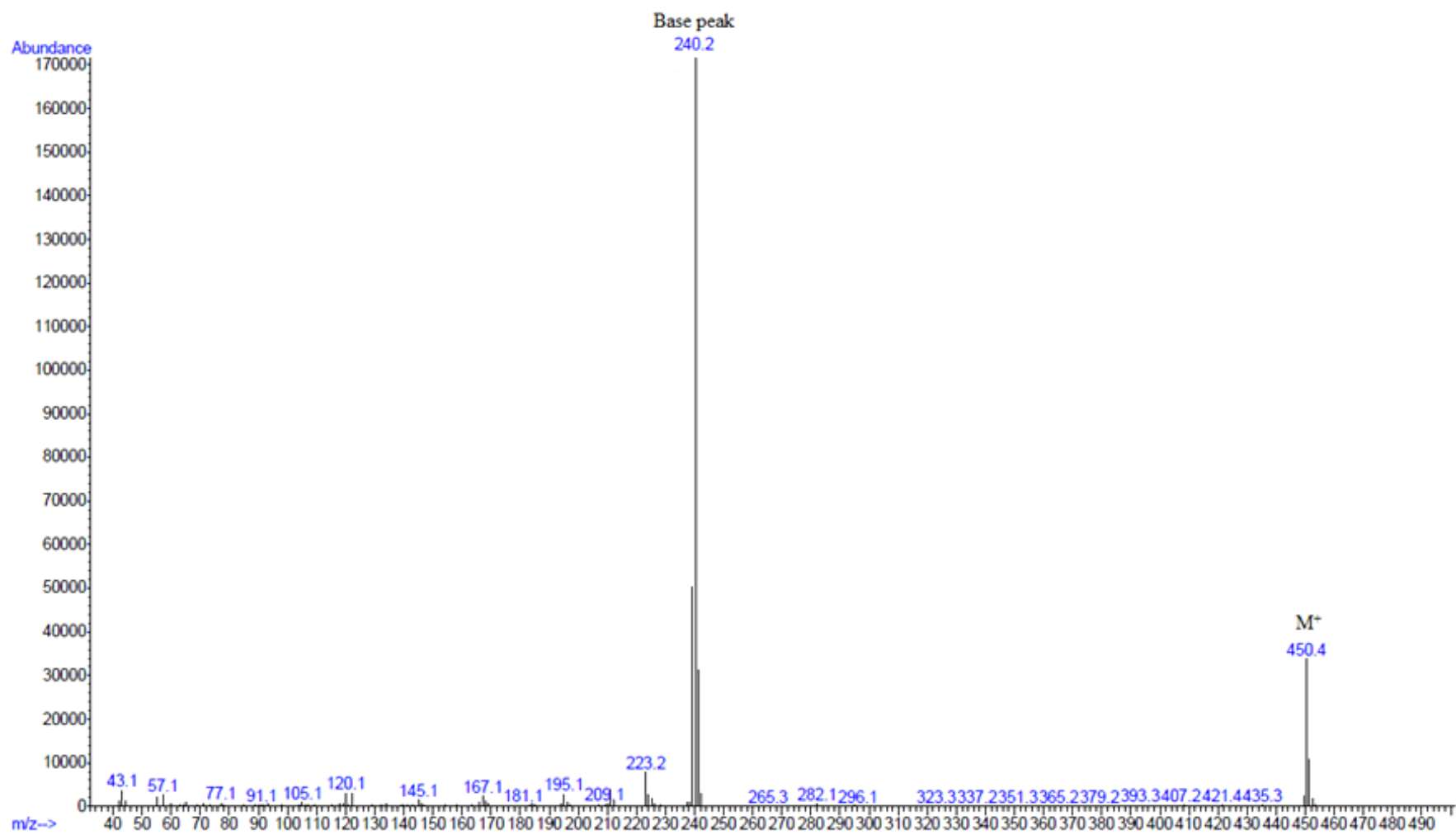


Figure 4.12: EI-mass spectrum of 14DMABAA

Simple removal of an electron from a molecule due to the bombardment of high-energy electrons in the ionisation chamber yields the molecular ion, M^+ whose weight is the actual molecular weight of the original molecule. The M^+ ion of **14DMABAA** appears at $m/z = 450.4$ and this value matches its theoretical molecular weight. The tallest peak or also called the base peak is observed at $m/z = 240.2$ which arises from $[N(CH_3)_2-C_6H_4-CH=N-C_6H_4-OH]^+$ ion, the most abundant ion in the ionisation chamber. This ion is gained by removing a neutral ketene molecule from the original molecule, giving rise to another peak at $m/z = 210.2$ (Hoffmann and Stroobant, 2007). The mechanism of fragmentation is shown in Figure 4.13.

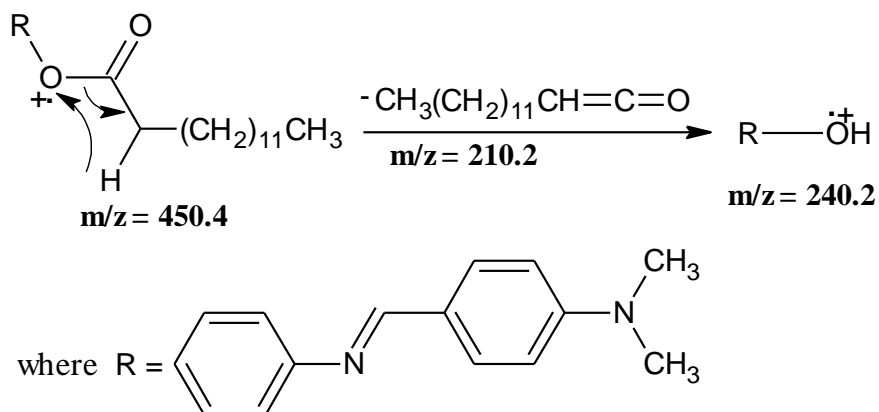


Figure 4.13: Mechanism of fragmentation for $[N(CH_3)_2-C_6H_4-CH=N-C_6H_4-OH]^+$ ion

A significant peak at $m/z = 223.2$ is due to the β -cleavage of carbonyl C-O bond, giving rise to $N(CH_3)_2-C_6H_4-CH=N-C_6H_4^+$ ion. The mechanism of fragmentation is shown in Figure 4.14.

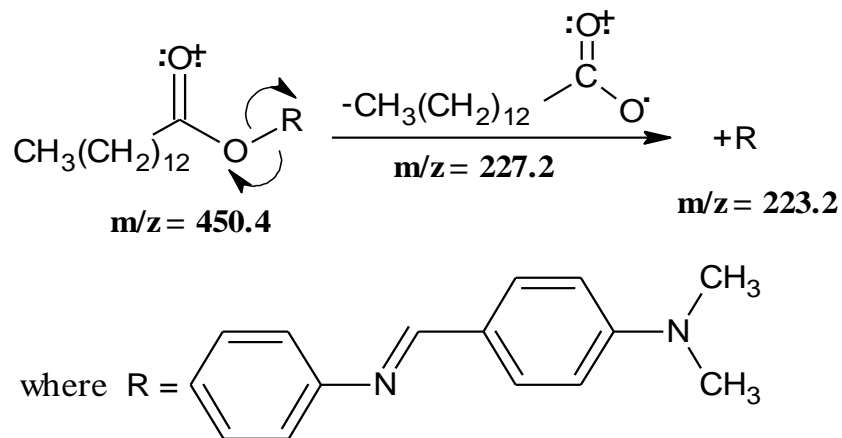


Figure 4.14: Mechanism of fragmentation for $\text{N}(\text{CH}_3)_2\text{C}_6\text{H}_4\text{-CH=N-C}_6\text{H}_4^+$ ion

For the peak at $m/z = 211.0$, the C-O bond of the carbonyl group undergoes α -cleavage to give rise to $\text{CH}_3(\text{CH}_2)_{12}\text{-C}^+=\text{O}$ ion. The mechanism of fragmentation is shown in Figure 4.15.

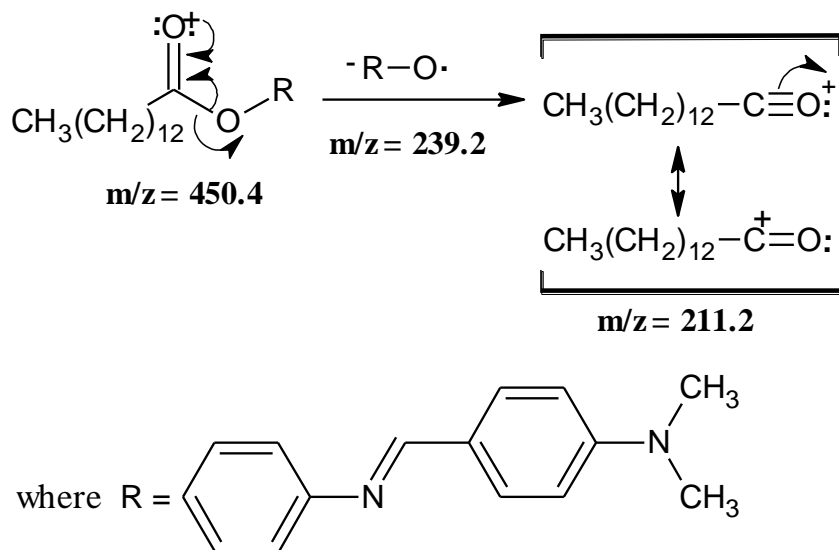


Figure 4.15: Mechanism of fragmentation for $\text{CH}_3(\text{CH}_2)_{12}\text{-C}^+=\text{O}$ ion

On the other hand, the α -cleavage of C-C bond of the imine linking group gives rise to $\text{N}(\text{CH}_3)_2\text{-C}_6\text{H}_4^+$ ion peak at $m/z = 120.1$. The mechanism of fragmentation is shown in Figure 4.16.

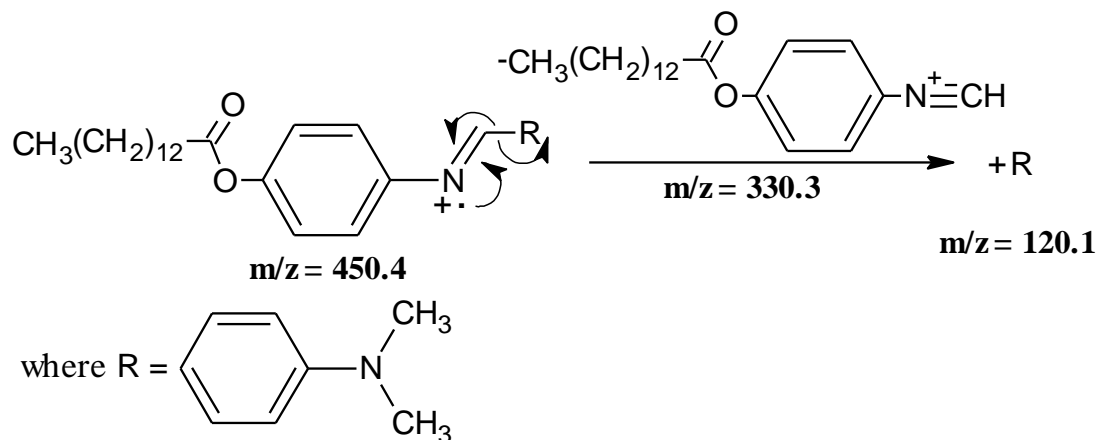


Figure 4.16: Mechanism of fragmentation for $\text{N}(\text{CH}_3)_2\text{-C}_6\text{H}_4^+$ ion

Lastly, there are two peaks observed at the lowest m/z region of the EI-mass spectrum which are most probably due to the α -cleavage of C-C bond in the long alkyl chain of myristic acid. They are $\text{CH}_3(\text{CH}_2)_3^+$ and $\text{CH}_3(\text{CH}_2)_2^+$ ion peak which can be observed at $m/z = 57.1$ and 43.1 , respectively. Their mechanisms of fragmentation are shown in Figure 4.17.

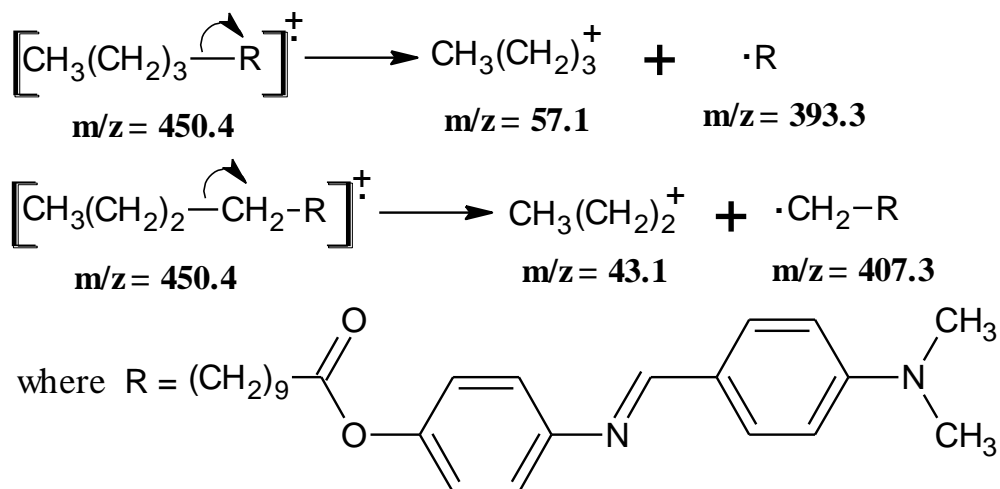


Figure 4.17: Mechanism of fragmentation for $\text{CH}_3(\text{CH}_2)_3^+$ and $\text{CH}_3(\text{CH}_2)_2^+$ ion

4.3 Mesomorphic Behaviour Analysis

4.3.1 Polarising Optical Microscopy Analysis of nDMABAA

The types of mesophases in **nDMABAA** series are identified using polarising optical microscopy (POM). All the compounds exhibited direct melting of the crystal phase to isotropic phase during the heating cycle. However, they exhibited exotherms characteristics of the isotropic-mesophase and mesophase-crystal transitions during cooling cycle, indicating the monotropic properties. Lower derivatives ($n = 6, 8$ and 10) exhibited only nematic phase, medium derivative ($n = 12$) exhibited co-existence of both nematic and smectic phases and higher derivatives ($n = 14, 16$ and 18) exhibited only smectic A phase. Optical photomicrographs of **10DMABAA**, **12DMABAA** and **14DMABAA** are shown in Figure 4.18 – 4.19 as representative illustrations.

When analysing mesophases by POM, the revealed texture depends on the alignment and phase structure of the sample. Generally, there are two basic forms of alignment for liquid crystalline compounds, homeotropic and homogeneous (planar). A homeotropic alignment is obtained when the long-axes of the molecules are normal to the surface of the glass plate. For such an orientation of molecules, the polarised light remains unaffected by the material and so the light cannot pass through the analyser, complete blackness is observed. In homogeneous (planar) alignment, the molecules have their long axes lying parallel or at an angle to the glass surface. With homogenous alignment, a thin

film of the mesophase exhibits birefringence and when viewed between crossed polarisers a coloured texture results. However, when the long molecular axes are in line with either polarisers, light is extinguished. In addition, the alignments are often dependent on the thickness of the sample. Thin samples tend to generate homeotropic alignment whereas thicker samples tend to generate both homeotropic and homogenous alignment (Singh and Dunmur, 2002d).

10DMABAA underwent transition from isotropic to nematic phase and finally to crystal phase during cooling process. The nematic phase was identified by the appearance of marble texture (Figure 4.18a) which containing some defect lines. Different areas of the sample appear quite uniform but slightly change in colour. Besides this, Brownian flashes (Figure 4.18b), a characteristic of the nematic phase was also observed before recrystallisation. This phenomenon happens due to the high degree of disorder of the nematic phase structure that induces high fluidity which in turn causing the dust particles within the samples to undergo intense Brownian motion (Collings and Hird, 1998c).

A remarkable characteristic was observed for **12DMABAA** where an additional smectic A phase with focal-conic fan texture (Figure 4.19b) along with some black homeotropic texture was observed after the formation of nematic phase with schlieren texture (Figure 4.19a) upon cooling cycle. The focal-conic fan texture of smectic A develops from nematic phase as batonnets that coalesce and eventually generate the focal-conic fan texture. The ellipses and hyperbolas of

the focal-conic fan texture appear as black lines in the texture because these are isotropic region where the sharp changes in the direction of the optic axis are found (Collings and Hird, 1998c). Further increase the alkyl chain to C14 did not show co-appearance of nematic and smectic A phases. **14DMABAA** exhibited only focal-conic fan texture (Figure 4.20) which indicates smectic A phase.

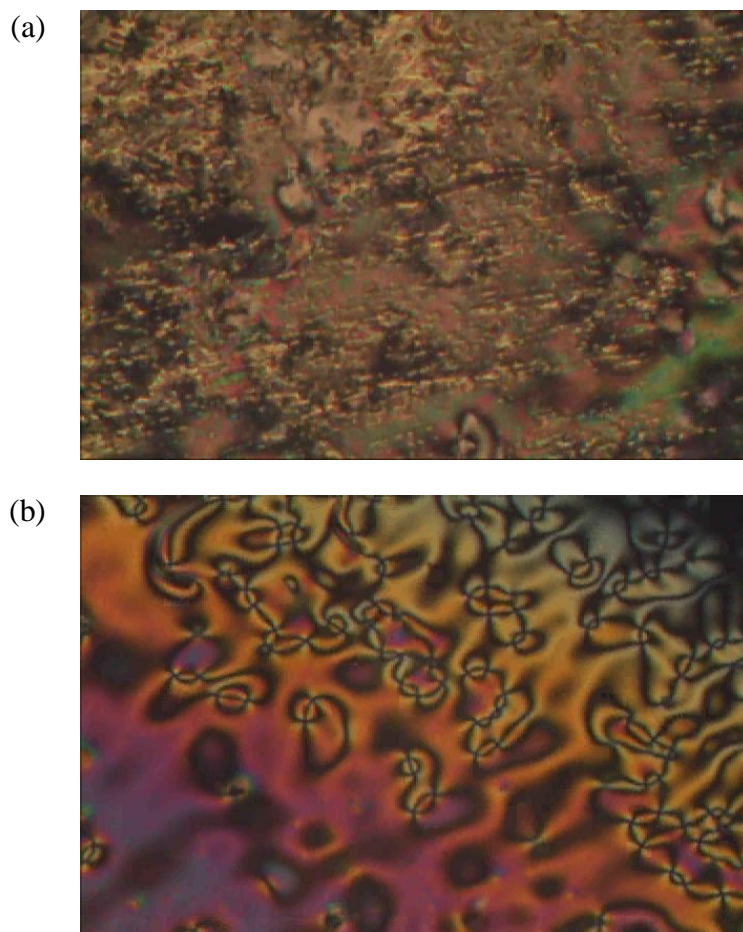


Figure 4.18: (a) Optical photomicrograph of 10DMABAA exhibiting nematic phase with marble and homeotropic textures during cooling cycle.

(b) Optical photomicrograph of 10DMABAA exhibiting Brownian flashes during cooling cycle.

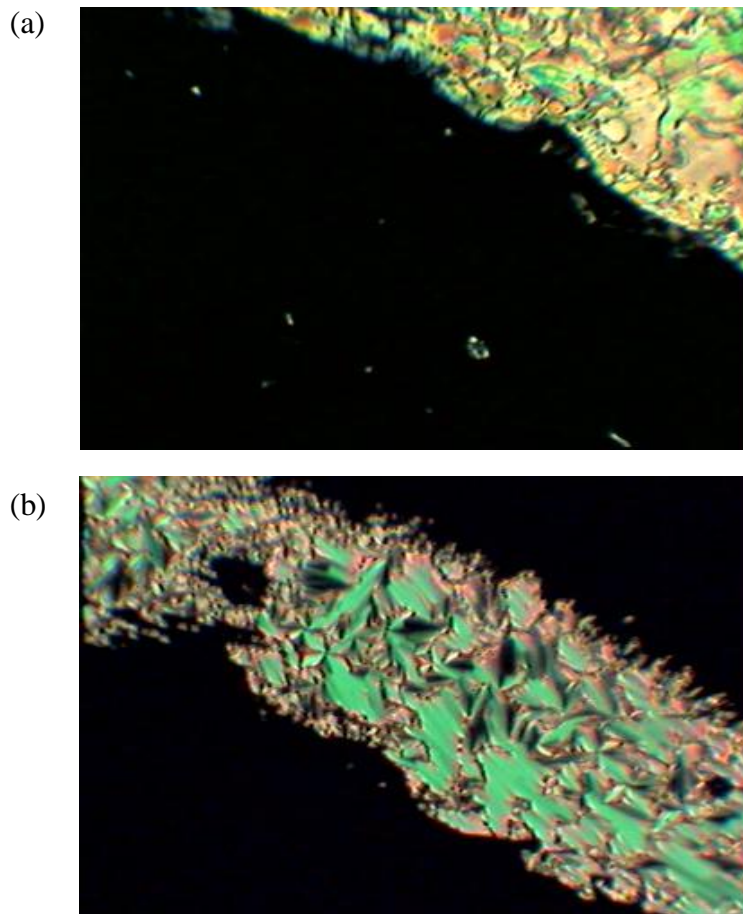


Figure 4.19: (a) Optical photomicrograph of 12DMABAA exhibiting nematic phase with schlieren and homeotropic (dark area) textures during cooling cycle
 (b) Optical photomicrograph of 12DMABAA exhibiting smectic A phase with focal-conic fan texture and homeotropic (dark area) textures during cooling cycle.

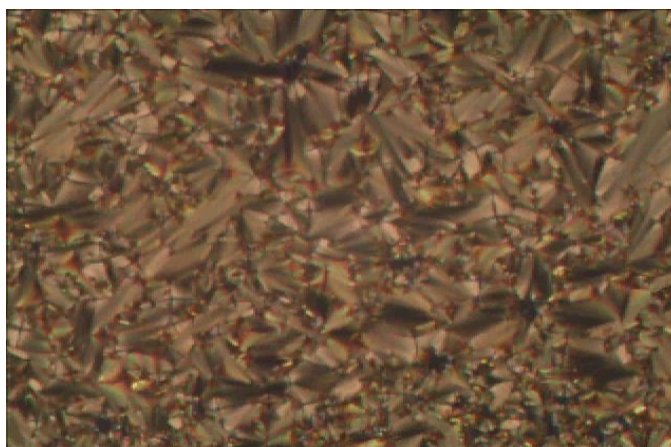


Figure 4.20: Optical photomicrograph of 14DMABAA exhibiting smectic A phase with focal-conic fan texture during cooling cycle.

4.3.2 Differential Scanning Calorimetry Analysis of nDMABAA

Differential scanning calorimetry (DSC) was used to reveal the presence of phase transitions in **nDMABAA** series by detecting the enthalpy change associated with each phase transition. The data of all the compounds in **nDMABAA** series are shown in Table 4.7 and the DSC thermogram of representative compound, **14DMABAA** is shown in Figure 4.21.

During heating cycle, an intense peak at 106.3 °C (38.86 kJ mol⁻¹) indicates the endothermic energy absorbed by the crystal molecules to break the intermolecular forces and change into isotropic phase. During cooling cycle, two peaks were observed. The relatively small peak at 94.0 °C (2.69 kJ mol⁻¹) represents the phase transition from isotropic to smectic A phase. Whereas, the larger peak at 89.7 °C (34.60 kJ mol⁻¹) represents the phase transition from smectic A to crystal phase. Crystallisation of the compound is an exothermic process and energy is released as its intermolecular forces are being formed.

Although the enthalpy changes at a transition cannot identify the types of phases associated with the transitions, the magnitude of the enthalpy change is proportional to the change in structural ordering of the phases involved (Collings, and Hird, 1998c). As observed in the cooling cycle of **14DMABAA**, the enthalpy changes of phase transition from isotropic to smectic A phase (2.69 kJ mol⁻¹) is much smaller than that from smectic A to crystal phase (34.60 kJ mol⁻¹). This

indicates that a considerable structural change is occurring in the latter phase transition. In other word, higher energy is released when the smectic A mesogens which are randomly arranged within the lamellar layers rearrange into a crystal phase with fixed position and orientation; strong intermolecular interactions are required to achieve such arrangement. Whereas, lower energy is released when the disoriented molecules in isotropic liquid rearrange to form the lamellar layers structure of smectic A phase. In addition, the melting points of all the monotropic mesogens of **nDMABAA** are higher than the clearing points, hence causing them to exhibit supercooling properties (Liu, 1981).

Table 4.7: Transition temperature and associated enthalpy changes upon heating and cooling of nDMABAA

Compound	Transition temperature, °C (enthalpy changes, kJ mol ⁻¹)						
	Cr	→	SmA	→	N	→	I
6DMABAA	.	-	-	-	-	108.6 (32.05)	.
	.	-	-	<i>91.3 (28.03)</i>	.	<i>97.2 (1.51)</i>	.
8DMABAA	.	-	-	-	-	109.8 (36.99)	.
	.	-	-	<i>87.7 (32.42)</i>	.	<i>94.4 (1.24)</i>	.
10DMABAA	.	-	-	-	-	110.1 (51.02)	.
	.	-	-	<i>84.3 (44.38)</i>	.	<i>94.5 (1.64)</i>	.
12DMABAA	.	-	-	-	-	104.8 (46.82)	.
	.	<i>88.3 (42.47)</i>	.	<i>92.5^a</i>	.	<i>93.3 (1.76)</i>	.
14DMABAA	.	-	-	-	-	106.3 (38.86)	.
	.	<i>89.7 (34.60)</i>	.	-	-	<i>94.0 (2.69)</i>	.
16DMABAA	.	-	-	-	-	108.2 (42.58)	.
	.	<i>93.6 (43.05)</i>	.	-	-	<i>96.6^a</i>	.
18DMABAA	.	-	-	-	-	109.4 (59.80)	.
	.	<i>94.6 (60.36)</i>	.	-	-	<i>99.4^a</i>	.

^a indicates POM data; values in italic are taken during cooling cycle

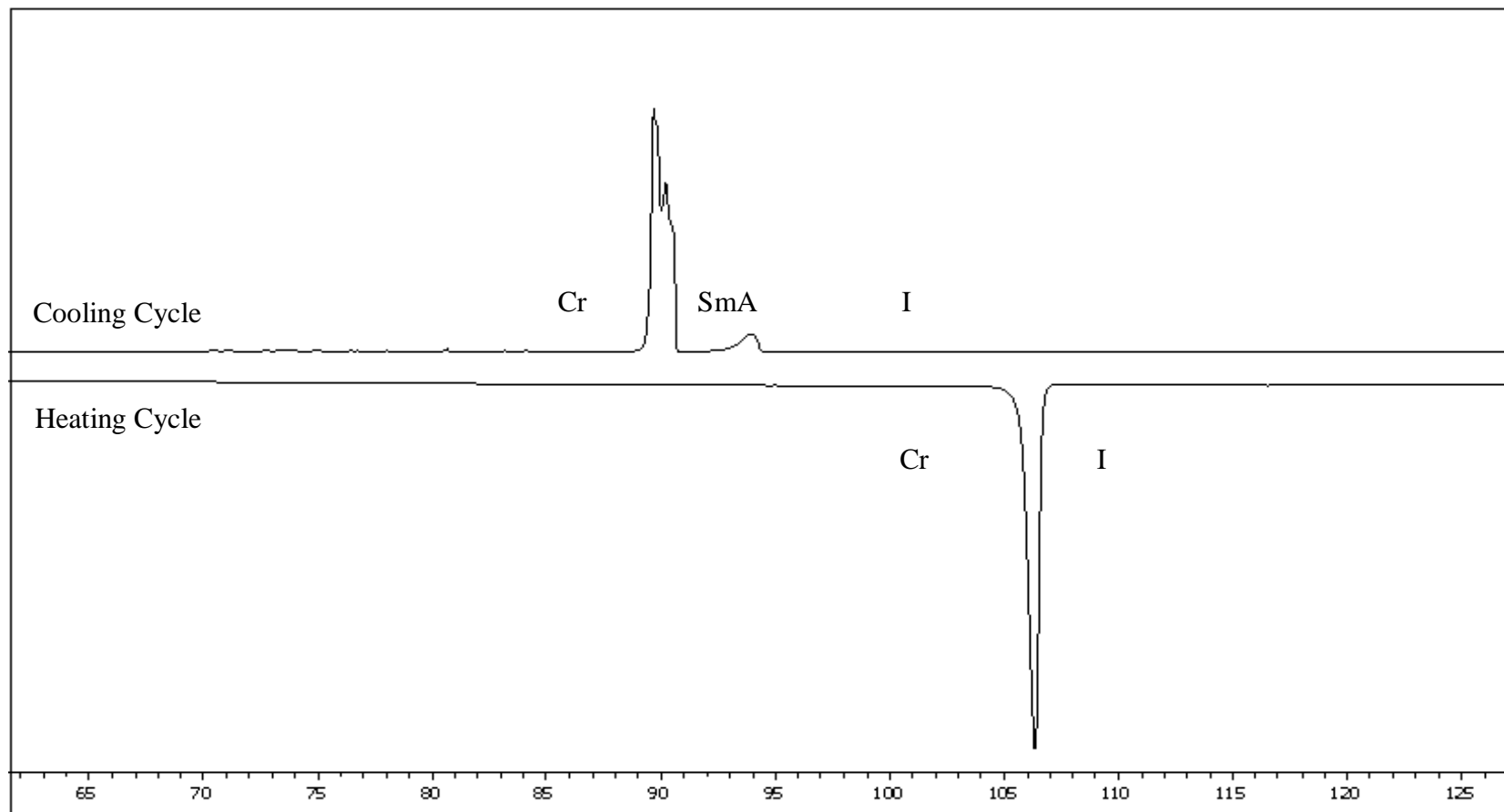


Figure 4.21: DSC thermogram of 14DMABAA

4.3.3 Effect of Alkyl Chain Length on Mesomorphic Properties

The plot of phase transition temperature against the length of alkanoyloxy chain of **nDMABAA** series during heating cycle is shown in Figure 4.22 and the data are shown in previous Table 4.7.

The melting temperatures increased from C6 to C10 derivatives, before showing a sudden drop at C12 derivative and then increased again from C12 to C18 derivatives. The ascending melting points could be attributed to the increase of Van der Waals attractive forces between the molecules when the alkyl chains length increases. On the other hand, the clearing temperatures exhibited a descending trend from C6 derivative to C12 derivative (except C10 derivative) due to the increase in the flexibility of the molecule induced by the longer alkyl chain, but when reaching certain length ($n \geq 12$), the excessive Van der Waals intermolecular forces of attraction increases the clearing temperatures again (Singh and Dunmur, 2002c).

By considering the chemical constitution of **nDMABAA** series, the emergence of nematic phase at the lower derivatives could have due to the branched methyl group terminal which disrupted the lamellar packing of smectic phase. Furthermore, the imine linking group (CH=N) which conferred a stepped core structure in which linearity is maintained, resulting in the thickening effect which in turn enhanced the nematic phase stability. However, the presence of

ester linking group in the structure tends to enhance the dipole-dipole interaction between molecules, facilitating the lateral packing and hence generating smectic phase (Collings and Hird, 1998b). In addition, the length of alkyl chains also plays an important role in determining the type of mesophase generated.

From the graph, it was observed that C6 to C10 derivative exhibited only nematic phase. As the length of the alkyl chain increased, co-existence of nematic and smectic A phase was observed for the C12 derivative. However, when the alkyl chain reaching certain length ($n \geq 14$), only the smectic A phase was induced. This suggests that the increase in the length of alkyl chain causes the nematic properties to decrease, in turn leading to enhancement of the smectic properties. This is because the attraction forces between the long alkyl chains leading to their intertwining which facilitates the lamellar packing required for smectic phase generation (Collings and Hird, 1998b). It can therefore be proposed that in order to generate smectic phase in the analogous substituted $C_6H_5CH=NC_6H_5$ compounds, the number of carbons in the alkanoyloxy chain must be at least 12.

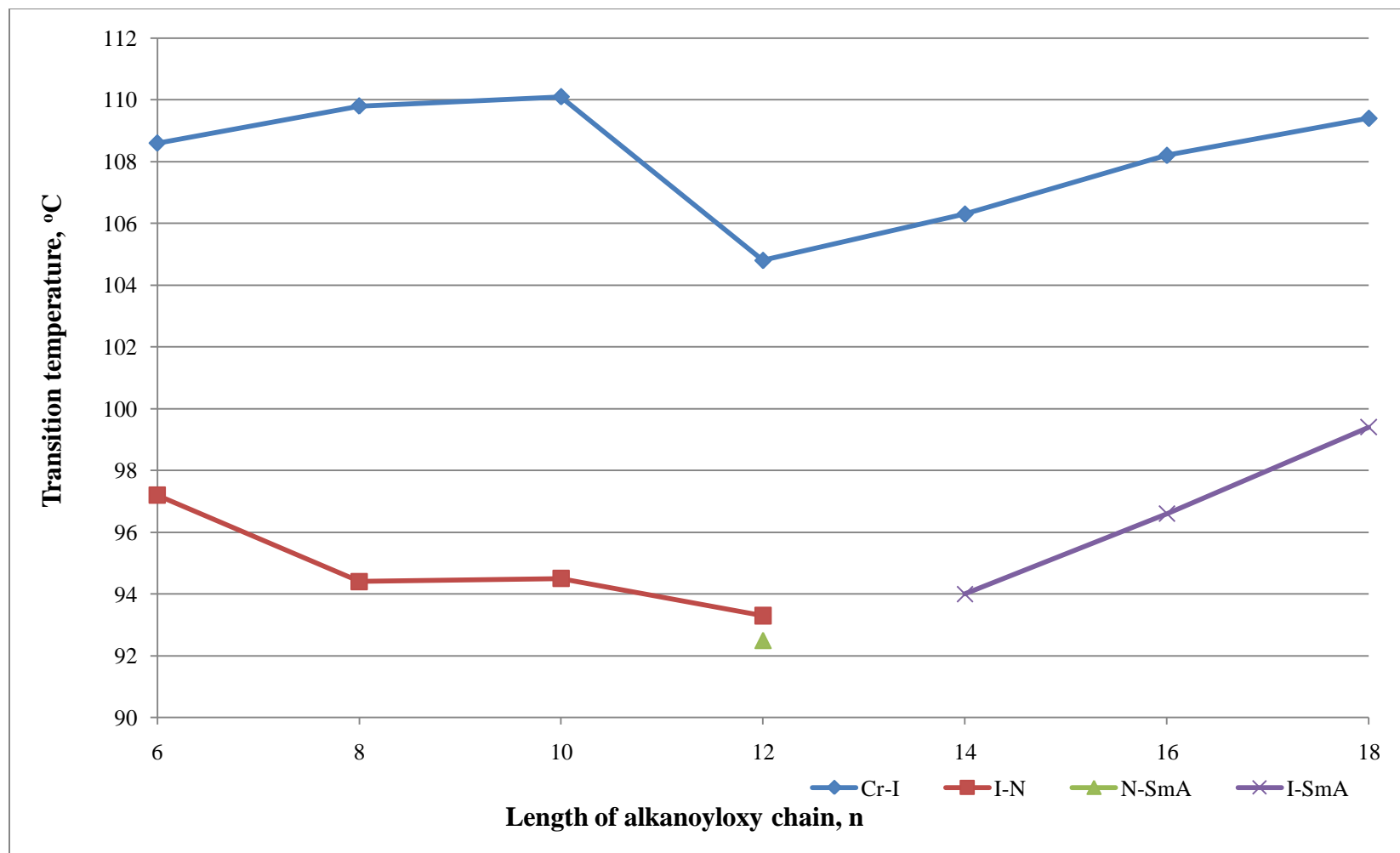
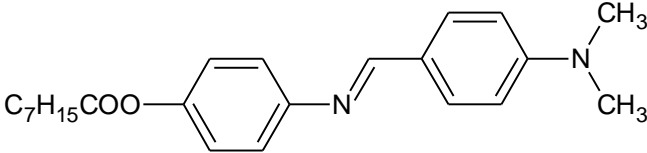
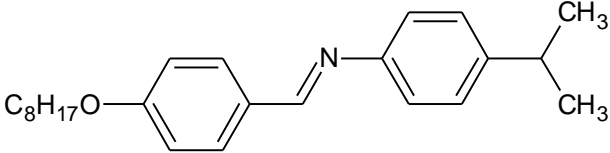
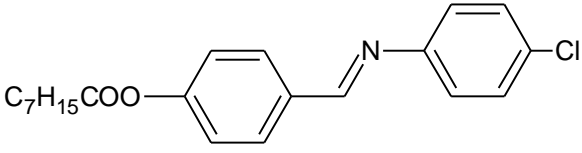
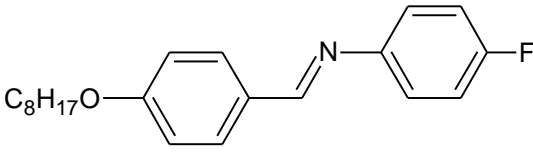


Figure 4.22: Plot of transition temperature versus the length of alkanoyloxy chain of nDMABAA series during heating cycle

4.4 Structural Comparison with Compounds Reported in the Literature

In order to study the structure-mesomorphic relationship, properties of **8DMABAA** (current study) and three other reported series, **IP-O8**, **8CIAB** and **8FAB** as tabulated in Table 4.8 were compared and discussed.

Table 4.8: Comparison of mesomorphic properties among structurally related compounds

Compound	Structure and phase transition (°C)	Reference
8DMABAA	 <p>Cr (87.4)^a N 108.6 I</p>	Current work
IP-O8	 <p>Cr 56.5 SmA 59.0 I</p>	(Vora <i>et al.</i> , 2001)
8CIAB	 <p>Cr (80.2)^a SmB 84.0 SmA 104.8 I</p>	(Ha <i>et al.</i> , 2010)
8FAB	 <p>Cr (55.1)^a SmB 62.2 SmA 65.2 I</p>	(Gandolfo <i>et al.</i> , 1988)

^a indicates monotropic phase

From the table, **8DMABAA** exhibits monotropic nematic phase while **IP-O8** exhibits enantiotropic smectic A phase. This is because of the high electronegativity of nitrogen atom in **8DMABAA** contributes to a stronger terminal intermolecular interaction which favours the formation of nematic phase. Despite the branching effect, the less electronegative carbon in isopropyl group of **IP-O8** still possess greater lateral interaction and thus prefers lamellar arrangement of smectic phase. Although the ester linking group in **8DMABAA** confers a stepped structure in which its linearity is maintained and such structure would tend to reduce the nematic phase stability due to the increased molecular breadth, the effect is minimized by the extended molecular length. The enhanced polarity due the π -electrons associated with the carbonyl group of the ester linking group increases the melting point and also facilitates the generation of nematic phase to a slight extent (Collings and Hird, 1998b).

8CIAB and **8FAB** have no branching terminal which disrupts the molecular packing and invariably reduces the mesophase stability like that in **8DMABAA** and **IP-O8**. This explains why both the **8CIAB** and **8FAB** exhibit high stability of smectic A and smectic B phase while **8DMABAA** does not exhibit any smectic phase and **IP-O8** exhibits only low stability of smectic A phase. The presence of two lateral methyl groups at the terminal position of **IP-O8** depressed its thermal stabilities and therefore having lower transition temperatures than **8CIAB** and **8FAB** which have not lateral substituents. Furthermore, thermal stability of **IP-O8** is also much lower compared to

8DMABAA. This is because the more polar nitrogen atom in **8DMABAA** enhances the molecular polarisability and hence increases the transition temperature (Collings and Hird, 1998b).

Both of the **8CIAB** and **8FAB** exhibited enantiotropic smectic A phase and monotropic smectic B phase. The incorporation of polar terminal substituent into a mesogen contributes to the molecular polarisability which can aid the lateral attraction between molecules and so generates a strong smectic character. The first member to exhibit smectic phase in both the **nCIAB** and **nFAB** series is the C4 derivatives. Hence, it can be proposed that in order to generate smectic phase in the analogous series, there must be at least four carbons in the alkyl chain. Besides that, the chlorine atom is larger than the fluorine atom and therefore more easily polarized due to the electrons surrounding the nucleus is far away and loosely held. Higher molecular polarisability contributed by the larger chlorine atom led to higher phase stability in **8CIAB**. Based on the same reasoning, the smaller and the less polarisable fluorine atom in **8FAB** caused its melting and transition temperature to be lower than that of **8CIAB**. In addition, the π -electrons associated with the carbonyl group in **8CIAB** also provide it greater intermolecular interactions among molecules and hence possessing higher melting and clearing temperatures (Demus *et al.*, 1998).

CHAPTER 5

CONCLUSION

A series of Schiff base esters, 4-(dimethylamino)benzylidene-4'-alkanoyloxyanilines (**nDMABAA**) containing different length of alkanoyloxy chain ($C_{n-1}H_{2n-1}COO^-$, $n = 6, 8, 10, 12, 14, 16, 18$) at the end of the molecules was successfully synthesized and characterised using FT-IR, 1H and ^{13}C NMR spectroscopy and EI-mass spectrometry. All the compounds are listed as below:

4-(Dimethylamino)benzylidene-4'-hexanoyloxyaniline (**6DMABAA**)

4-(Dimethylamino)benzylidene-4'-octanoyloxyaniline (**8DMABAA**)

4-(Dimethylamino)benzylidene-4'-decanoyloxyaniline (**10DMABAA**)

4-(Dimethylamino)benzylidene-4'-dodecanoyloxyaniline (**12DMABAA**)

4-(Dimethylamino)benzylidene-4'-tetradecanoyloxyaniline (**14DMABAA**)

4-(Dimethylamino)benzylidene-4'-hexadecanoyloxyaniline (**16DMABAA**)

4-(Dimethylamino)benzylidene-4'-octadecanoyloxyaniline (**18DMABAA**)

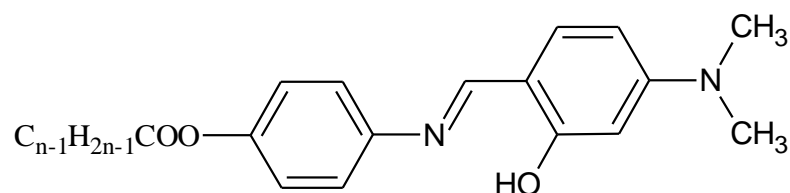
The IR spectral analysis of **nDMABAA** confirmed the presence of C-H, C=O, C=N, C=C, C-N, C-O and COO- functional groups. In the 1H NMR spectral analysis of representative compound, **14DMABAA**, the emergence of azomethine proton (CH=N) peak at $\delta = 8.33$ ppm indicated that the imination process was a success. In ^{13}C NMR spectral analysis of **14DMABAA**, the azomethine (C=N), carbonyl (C=O) and dimethylamino [$C(NH_3)_2$] carbons have been successfully

assigned too. In Mass spectrometry analysis of **14DMABAA**, the molecular ion peak and the base peak were observed at $m/z = 450.4$ and 240.2 , respectively.

The mesomorphic properties were investigated by using POM and DSC. Under POM, All derivatives of **nDMABAA** showed monotropic behaviour whereby mesophases were observed during cooling cycle only. Lower derivatives ($n = 6, 8$ and 10) exhibited only nematic phase, medium derivative ($n = 12$) exhibited co-existence of both nematic and smectic A phases and higher derivatives ($n = 14, 16$ and 18) exhibited only smectic A phase. Nematic phase and smectic A phases were identified by the presence of schlieren or marble and focal-conic fan textures, respectively. As the alkyl chain length increases, the tendency for smectic phase to emerge increases and eventually eliminate the nematic phase. This is due to the attraction forces between the long alkyl chains leading to their intertwining which facilitates the lamellar packing required for smectic phase generation. DSC further confirmed the presence of phase transitions of the compounds observed under POM by detecting the enthalpy changes associated with each phase transition. The DSC thermogram of representative compound, **14DMABAA** showed only one peak at $106.3\text{ }^{\circ}\text{C}$ (38.86 kJ mol^{-1}) during heating cycle that can be ascribed to direct isotropization process (Cr-to-I) and two peaks at $94.0\text{ }^{\circ}\text{C}$ (2.69 kJ mol^{-1}) and $89.7\text{ }^{\circ}\text{C}$ (34.60 kJ mol^{-1}) during cooling cycle which represent the phase transitions (I-to-SmA) and (SmA-to-Cr) respectively.

Further Study

In further study, a hydroxyl group (-OH) can be added to benzylidene aromatic ring, at the *ortho* position of the azomethine group. The hydroxyl group will tend to increase the molecular polarisability anisotropy which in turn increases the degree of molecular order, and the Van der Waals forces between molecules, enhancing the stability of smectic phase.



where

n = 6, 8, 10, 12, 14, 16, 18

REFERENCES

Journal:

- Al-Hamdani, U. J., Gassim, T. E. and Radhy, H. H. (2010). Synthesis and Characterization of Azo Compounds and Study of the Effect of Substituents on Their Liquid Crystalline Behavior. *Molecules*, 15, 5620-5628.
- Belmar, J. (1999). New Liquid Crystals Containing the Benzothiazol Unit: Amides and Azo Compounds. *Liquid Crystals*, 26: 3, 389-396.
- Chandrasekhar, S., Sadashiva, B. K. and Suresh, K. A. (1977). Liquid Crystals of Disc-like Molecules. *Pramana*, 9, 5, 471-480.
- Dziaduszek, J., Dabrowski, R. and Gauza, S. (2009). Synthesis and Mesomorphic Properties of Laterally Fluorinated Phenyl Isothiocyanatotolanes and Their High Birefringent Mixtures. *Opto-Electron. Rev.*, 17, 20-24.
- Galewaki, Z. and Coles, H. J. (1999). Liquid Crystalline Properties and Phase Situation in 4-chlorobenzylidene-4'-alkylanilines. *J. Mol. Liq.*, 79, 77-87.
- Godzwan, J., Sienkowska M. J. and Galewski, Z. (2007). Smectic Polymorphism of 4-decyloxybenzylidene-4'-alkyloxyanilines and Their Mixture with polar standards of mesophases. *Phs. Trans.*, 80(3), 1029-0338.

- Gray, G.W., Hogg, C. and Lacey, D. (1981). The Synthesis and Liquid Crystal Properties of Some Laterally Fluorinated Trans – Cyclohexane – 1 - Carboxylate and Benzoate Esters. *Mol. Cryst. Liq. Cryst.*, 67, 1-24.
- Ha, S. T., Ong, L. K., Sivasothy, Y., Yeap, G. Y., Lin, H. C., Lee, S. L., Boey, P. L. and Bonde, N. L. (2010). Mesogenic Schiff Base Esters with Terminal Chloro Group: Synthesis, Thermotropic Properties and X-ray Diffraction Studies. *Int. J. Phys. Sci.*, 5(5), 564-575.
- Kelker, H. and Scheurle, B. (1969). A Liquid Crystalline (Nematic) Phase with a Particularly Low Solidification Point. *Angew. Chem. Int. Edn.*, 8: 884- 885.
- Liu, C. T. (1981). Molecular Structure and Phase Transition of Thermotropic Liquid Crystals. *Mol. Cryst. Liq. Cryst.*, 74: 25-37.
- Luzzati, V., Mustacchi, H. and Skoulios, A. (1957). Structure of the Liquid Crystal Phases of the Soap-water System: Middle soap and Neat soap. *Nature*, 180, 600-601
- Madsen, L. A., Dingemans, T. J., Nakata, M., and Samulski, E. T. (2004). Thermotropic Biaxial Nematic Liquid Crystals. *Phys, Rev, Lett.*, 92, 145505.
- Marcos, M., Melendez, E. and Serrano, J.L. (1983). Synthesis and Mesomorphic Properties of Three Homologous Series of 4,4'-dialkoxy- α,α' -dimethylbenzalazines. *Cryst. Liq. Cryst.*, 91, 157-172.

- Narasimhaswamy, T. and Srinivasan, KSV. (2004). Synthesis and Characterisation of Novel Thermotropic Liquid Crystals Containing a Dimethylamino Group. *Liq. Cryst.*, 31, 1457-1462.
- Neises, B. and Steglich, W. (1978). Simple Method for the Esterification of Carboxylic Acids. *Angew. Chem. Int. Ed.*, 17, 522-524.
- Prajapati, A. K. and Bonde, N. L. (2009). Mesogenic benzothiazole derivatives with a polar nitro substituent. *Mol. Cryst. Liq. Cryst.*, 501: 72-85.
- Regoa, J. A., Harvey, J. A. A., MacKinnon, A. L. and Gatdula E. (2010). Asymmetric Synthesis of a Highly Soluble 'Trimeric' Analogue of the Chiral Nematic Liquid Crystal Twist Agent Merck S1011. *Liq. Cryst.*, 37, 1, 37-43.
- Schroeder, D. C. and Schroeder, J. P. (1976). Liquid Crystals. 6. Mesomorphic Phenols and Primary Amines. p-Phenylene Dibenzoates with Terminal Hydroxy and Amino Groups. *J. Org. Chem.*, 41 (15), 2566–2571.
- Thaker, B. T., Patel, P., Vansadia, A. D. and Patel, H. G. (2007). Synthesis, Characterization, and Mesomorphic Properties of New-Crystalline Compounds Involving Ester-Azomethine Central Linkages, Lateral Substitution, and a Thiazole Ring. *Mol. Cryst. Liq. Cryst.*, 466, 13-22
- Vora, R., Prajapati, A. and Kevat, J. (2001). Effect of Terminal Branching on Mesomorphism. *Mol. Cryst. Liq. Cryst.*, 357, 229-237.

Yeap, G. Y., Ha, S. T., Lim, P. L., Boey, P. L., Ito, M. M., Sanehisa, S. and Vill, V. (2006). Nematic and Smectic A Phases in Ortho-hydroxy-para-hexadecanoyloxybenzylidene-para-substituted Anilines. *Mol. Cryst. Liq. Cryst.*, 452, 63-72.

Book Chapter:

Chandrasekhar, S. (1992). Introduction. In: *Liquid Crystals*. 2nd Edition. (pp 1-14). Cambridge: Cambridge University Press.

Collings, P. J. (2002). What Are Liquid Crystal. In: *Liquid Crystals: Nature's Delicate Phase of Matter*. 2nd Edition. (pp 1-17). United Kingdom: Princeton University Press.

Collings, P. J. and Hird, M. (1998a). Introduction to a Special Phase of Matter. In: *Introduction to Liquid Crystal Chemistry & Physics*. (pp 1-16). London: Taylor and Francis.

Collings, P. J. and Hird, M. (1998b). Calamitic Liquid Crystals-Nematic and Smectic Mesophases. In: *Introduction to Liquid Crystal Chemistry & Physics*. (pp 43-77). London: Taylor and Francis.

Collings, P. J. and Hird, M. (1998c). Identification of liquid crystal phases – mesophase characterization. In: *Introduction to Liquid Crystal Chemistry & Physics*. (pp 177-188). London: Taylor and Francis.

- Demus, D., Goodby, J., Gray, G. W., Spiess, H. W. and Vill, V. (1998). Chemical Structure and Mesogenic Properties. In: *Handbooks of Liquid Crystals*. Vol 1: Fundamentals. (pp 133-153). Weinheim, New York, Chichester, Brisbane, Singapore, Toronto: Wiley-VCH.
- Dierking, I. (2003). Introduction. In: *Textures of Liquid Crystals*. (pp 1-16). United Kingdom: Wiley-VCH.
- Fisch, R. M. (2006). Liquid Crystals. In: *Liquid Crystals, Laptops and Life*. (pp 163-182). United State of America: World Scientific.
- Hoffmann, E. and Stroobant, V. (2007). Fragmentation Reactions. In: *Mass Spectrometry Principles and Applications*. 3rd Edition. (pp 273-298). England: John Wiley & Sons.
- Lam, C. K. (2007). Introduction to Liquid Crystals. In: *Liquid Crystals*. 2nd Edition. (pp 1-7). Canada: John Wiley & Sons.
- Pavia, D. L., Lampman, G. M., Kriz, G. S. and Vyvyan, J. R. (2009a). Infrared Spectroscopy. In: *Introduction to Spectroscopy*. 4th Edition. (pp 52-76). United State of America: Brooks/ Cole, Cengage Learning.
- Pavia, D. L., Lampman, G. M., Kriz, G. S. and Vyvyan, J. R. (2009b). Nuclear Magnetic Resonance Spectroscopy. In: *Introduction to Spectroscopy*. 4th Edition. (pp 102-194). United State of America: Brooks/ Cole, Cengage Learning.

- Solomons, T. W. G. and Fryhle, C.B. (2000). Amines. In: *Organic Chemistry*. 7th Edition. (pp 960-961). New York, Chichester, Weinheim, Brisbane, Singapore, Toronto: John Wiley & Sons.
- Stegemeyer, H. (1994a). Phase Types, Structures, and Chemistry of Liquid Crystals. In: *Liquid Crystals*. (pp 1–49). New York: Steinkopff Darmstadt Springer.
- Stegemeyer, H. (1994b). Liquid Crystal Displays. In: *Liquid Crystals*. (pp 195–203). New York: Steinkopff Darmstadt Springer.
- Singh, S. and Dunmur, D. A. (2002a). Liquid Crystals: Main Types and Classification. In: *Liquid Crystals: Fundamentals*. (pp 1-23). Singapore: World Scientific Publishing.
- Singh, S. and Dunmur, D. A. (2002b). Lyotropic Liquid Crystals. In: *Liquid Crystals: Fundamentals*. (pp 453-457). Singapore: World Scientific Publishing.
- Singh, S. and Dunmur, D. A. (2002c). Nematic Liquid Crystals. In: *Liquid Crystals: Fundamentals*. (pp 94-108). Singapore: World Scientific Publishing.
- Singh, S. and Dunmur, D. A. (2002d). Defects and Textures in Liquid Crystals. In: *Liquid Crystals: Fundamentals*. (pp 471-481). Singapore: World Scientific Publishing.

WebPages:

Mohanty, S. (2003). Liquid Crystals – The ‘Fourth’ Phase of Matter. URL:

<http://www.ias.ac.in/resonance/Nov2003/pdf/Nov2003p52-70.pdf>.

Accessed on 12th December 2010.

Parbhoo, R. (2008). A chemical Engineer’s Guide to Cleaning Just About

Anything. URL: <http://illuminate.usc.edu/article.php?articleID=168>.

Accessed on 15th December 2010.

McMichael, K (2001). Amines: Reactions. In: *Organic Chemistry Pages*.

Washington State University. URL:

<http://chemistry2.csudh.edu/rpendarvis/aminrxn.html>.

Accessed on 20th January 2010.